We are IntechOpen,
the world's leading publisher of
Open Access books
Built by scientists, for scientists

6,900
Open access books available

186,000
International authors and editors

200M
Downloads

Our authors are among the

154
Countries delivered to

TOP 1%
most cited scientists

12.2%
Contributors from top 500 universities

CLARIVATE ANALYTICS

BOOK CITATION INDEX

INDEXED

WEB OF SCIENCE™

Selection of our books indexed in the Book Citation Index
in Web of Science™ Core Collection (BKCI)

Interested in publishing with us?
Contact book.department@intechopen.com

Numbers displayed above are based on latest data collected.
For more information visit www.intechopen.com

Simulating Odour Dispersion about Natural Windbreaks

Barrington Suzelle, Lin Xing Jun and Choiniere Denis
Department of Bioresource Engineering, Macdonald Campus of McGill University,
Consumaj inc.
Canada

1. Introduction

Worldwide, population and economic growth has reduced the distance separating residential areas and odour sources. Annoyance can result from not only obnoxious odours but also prolonged pleasant odours such as produced by a chocolate or frying factory. Odours indirectly affect human health through stress (Evans & Cohens, 1987) and their impact is greater when humans are exposed to a continuous rather than an intermittent source. People with a problem coping style (seeking a solution to the odour problem) can become more annoyed by odours than those using comforting cognition (telling themselves that the situation will improve) or having an emotional oriented style (those looking for a diversion) because the solution is often out of hand (Cavalini et al., 1991). Although pleasant odours can become annoying when too concentrated or persistent, malodours are perceived as unpleasant under most if not all conditions. Malodours are also known to activate a different area of the brain, as compared to pleasant odours (Zald & Pardo, 2000). According to Jacob et al. (2003), the response of humans to malodours is quite consistent and it differs compared to that of pleasant odours which produce a wider range of response. Furthermore, Jacob et al. (2003) found that the detection of any odour increases with dose and duration, but that the change in response of humans is much more important for small increases of malodour concentrations when presented at a low level just above their detection threshold.

Accordingly, odour dispersion models must take into consideration the olfactory response of humans. Noxious odours are likely much easier to model because most humans will classify them as an annoyance, as opposed to pleasant odours where the response is more variable. Furthermore, the human olfactory sense will detect the presence of an odour at a low level and if noxious, will immediately classify it as a nuisance. As the air concentration of the odorous gas increases, the relative level of annoyance does not increase as quickly. Furthermore, at a specific odorous gas air concentration, the response becomes intolerable and increasing the concentration any further will not increase the level of annoyance. To be accurate, this type of response must be incorporated into an odour dispersion model.

The use of separation or setback distances for odour sources conveniently insures the dilution of malodours to acceptable levels in the vicinity of neighbours (Redwine & Lacey, 2000). Nevertheless, conventional separation distances rely on the generalized odour

emission associated with a given operation regardless of management issues. Accordingly, separation distances do not provide satisfactory legislation against nuisance in many instances (Jacobston et al., 2005). Effective separation distances need to consider a greater number of factors pertaining to odour emission rate and character, and subsequent dispersion before reaching the neighbours. Furthermore, management practices can change the cleanliness of the operation, the frequency and intensity of odour emissions and the location of the source on the property (Li & Guo, 2008; Le et al., 2005; Lim et al. 2001). Physical and climatic factors constitute other factors, namely topography and buildings, and atmospheric stability, air temperature, and wind velocity and direction (Schauberger et al., 1999; Zhu et al. 2000; Lin et al., 2007c, 2009a,b).

To improve the calculation of separation distances, several industrial models were modified for agricultural applications. The first models where steady state and Gaussian based (Chen et al., 1998; Smith & Watts, 1994) with a normally distributed exponential function extrapolated to ground level. Examples of such models are the ISCST3 and AUSPLUME. Later, McPhail (1991) and Gassman (1993) suggested that odours should be modelled as a series of puffs, to produce cycles of strong followed by weaker odour concentrations. An example of such models is INPUFF2, which is Gaussian based and is capable of simulating the release of odours over short intermittent periods. Zhu et al. (2000) tested this model in the Canadian Prairie Provinces with swine operations and resident panellists trained to compare odour annoyance against the n-butanol scale (ASTM 1999). Whereas the accuracy was relatively high up to a distance of 300 m from the source, INPUFF2 performed poorly at distances exceeding 400 m, where simulation was critical in determining the annoyance limit of the odour plume. Furthermore, the odour source emission rate needed to be scaled up by a factor of 35 and 10, for odours from livestock shelters and manure storages, respectively. CALPUFF is another Gaussian dispersion model simulating the dispersion of odours released over short time intervals, but with the added advantage of a Lagrangian function simulating the effect of spatially variable wind conditions. Xing et al. (2006) evaluated CALPUFF along with three other models, using once more panellists trained to recognize odour intensity using the n-butanol scale. The agreement between measured field data and the four models ranged between 37 and 50 %.

Computational Fluid Dynamics models have successfully simulated gas dispersion in complex spaces (Riddle et al., 2004), such as ammonia distribution in barns (Sun et al., 2002) and spray droplet transport in fields (Ucar & Hall, 2001). Lin et al. (2007b, 2009a, b) produced a model based on Computational Fluid Dynamics (CFD) to simulate odour dispersion downwind from natural windbreaks. The model was calibrated with field odour observations using panellists trained to associate odour concentration with an odour annoyance scale of 0 to 10, where 10 is the maximum level of annoyance. The CFD model required as input, the exponential equation correlating odour annoyance and concentration, as perceived by the panellists in an olfactory laboratory, after each morning of field measurements. The R^2 exceeded 0.75 when all the data beyond 150 m was considered, as these observation points corresponded to odour concentration below 117 OU m^{-3} and within the annoyance scale of 1 to 10. For odour concentrations exceeding 117 OU m^{-3}, the panellists were assigning the maximum annoyance level of 10, irrespective of the odour concentration value. In contrast, the n-butanol scale uses an odour intensity scale of 1 for 25 OU m^{-3}, of 2 for 72 OU m^{-3}, and so on up to 1834 OU m^{-3} for a scale of 5 (Guo et al., 2001). Accordingly, the n-butanol scale is designed to measure high odour concentration levels

whereas the method used by Lin et al. (2007b, 2009a, b) is designed to measure odour levels in the vicinity of the threshold values. In determining separation distances, the threshold values can be most useful.

Windbreaks were suggested in the late 1990's as a possible odour dispersion technique. Based on Asian research demonstrating the successful reduction of odours, North American livestock producers have used natural and artificial windbreaks on the fan side of livestock shelters to reduce odours emissions. The effect of a porous wall was studied by means of smoke emitters and simulated using a Gaussian model (Bottcher et al., 2000; Bottcher et al., 2001). The porous wall was found to vertically divert the odours from the exhaust fans and promote mixing with the wind flowing over the building, but not to be as effective as tall stacks. In Asia, solid walls have been used around livestock barns to precipitate dust released by the ventilation system (Bottcher, 2000). Dust has been shown to carry odours (Das et al., 2004). Such application requires a windbreak with a high porosity capable of reducing wind velocity and turbulence. The same principle has been applied to control snow and sand accumulation, reduce pesticide drift, increase crop yield and reduce heat losses from animals and buildings (Plate, 1971; Heisler & Dewalle, 1988; Wang & Takle, 1997; Ucar & Hall, 2001; Guan et al., 2003; Vigiak et al., 2003; Wilson & Yee, 2003a). Accordingly, several North American cooperative extension services offer information on planting natural windbreaks or tree shelter belts, suggesting a high porosity in the absence of solid scientific testing.

The objective of the present chapter is therefore to present the development of a model simulating the dispersion of odours or the size of the odour plume formed downwind from a natural shelter belt or windbreak located at a specific distance from an odour source. The purpose of the model was to identify the best management practices for the implementation of natural windbreaks minimizing the size of the odour plume; best management practices pertain to the properties of the windbreak itself, its location with respect to the odour source and the general climatic environment for the given region. The model uses Computational Fluid Dynamics (CFD) to estimate the size and intensity of the odour plume to establish the necessary separation distance between the source and the neighbouring receptor susceptible to annoyance. The model development includes the selection of a computational method capable of handling conditions of high turbulence, the addition of an olfactory perception equation and finally the output validation.

In summary and with the windbreak dispersion model developed, this Chapter will examine the features of natural windbreaks which enhance atmospheric dispersion and maximize the reduction in odour plume length. Finally, this Chapter will examine the effect of various climatic conditions on the performance of windbreak and their effectiveness in shortening odour plumes.

2. Field acquisition of calibrating and validating data

Field odour dispersion data was required to calibrate and validate the model. As well, typical natural windbreak characteristics were required to establish equations for its physical description. The field work therefore consisted in producing an odour generator which could generate an odorous air stream from a single point. Then, 5 sites were used to measure odour plumes under different climatic conditions: 1 control site without a windbreak, and 4 sites where the windbreaks offered different combinations of tree type, dimension and porosity. The distance between the odour generator and the windbreak were

also varied. In all, 39 different field tests were conducted to obtain data for the calibration and validation of the model.

2.1 The field instruments

A mobile odour generator was designed and built to be able to produce, in the field, a controllable level of odour emissions during the experiment (Lin et al., 2006). The odour generator consisted of a 500 L tank filled with swine manure (Fig. 1). A pump provided a consistent flow of manure over a vertical porous filter through which air was blown at a rate of 1.65 $m^3 s^{-1}$. The odour generator offered an air/liquid contact surfaced of 76.8 m^2.

During all field tests, the released odorous air was sampled at regular 30 minute intervals using Alinfan® bags. A laboratory forced choice dynamic olfactometer was then used to establish the threshold dilution value of each air samples by the same 12 trained panellists who observed the field odour plume dispersion. Odour concentration (OC) was expressed as "odour units per cubic meter" (OU m^{-3}) (CEN, 2001; Schauberger et al., 2002; Zhang et al., 2002). The rate of odour production, OU s^{-1}, was computed using the air flow rate of the odour generator.

Fig. 1. The odour generator carried on a truck to be positioned at specific distances upwind from the windbreak (Lin et al., 2006)

During each field test and installed on a 7.6 m high tower, a weather station was positioned 200 m upwind from the windbreak to avoid disturbance. At one minute intervals, a

computer recorded the temperature, wind direction and wind speed. The wind direction was measured before hand to estimate the range of the field odour plume and to direct panellists into the odour plume zone. Air stability values were obtained from the weather station at the Pierre Elliott Trudeau Airport (Montreal, Canada) located 50 km north of the field sites. This weather station was the nearest measuring Pasquill-Gifford atmospheric stability conditions.

2.2 The experimental windbreaks

This experiment was conducted using 4 uniform single row natural windbreaks located at least 5 km away from any livestock operation to eliminate interferences (Table 1; Fig. 2). The porosity of each windbreak was optically evaluated by measuring the percentage of open surface visible through the windbreak (Heisler and Dewalle, 1988; Guan et al., 2003).

Each natural windbreak was different in terms of porosity, tree type and height (Lin et al., 2006). The optical porosity of the windbreaks on sites 1 and 3 was 0.55 compared to 0.35 for those on sites 2 and 4 (Table 1). The windbreaks on sites 1 and 2 were of deciduous trees as compared to conifers for those on sites 3 and 4. All sites were located on farm land with a relatively flat and consistent slope of 0.1 % and the vegetation did not exceed a height of 0.7 m. Tree height was the other parameter which varied among windbreaks, sites 1 and 4 offering windbreaks with a height exceeding 15 m compared to sites 2 and 3 offering windbreaks with a height under 10 m. A control site (site 5) without windbreak was selected to also observe odour dispersion. This site consisted of relatively flat (0.1 % uniform slope) land without trees or fences, where a cereal crop had been freshly harvested.

2.3 The panelists and the olfactomètre

For the field tests and the laboratory olfactory work, three groups of four panellists were trained by requiring them to detect n-butanol at concentrations of 20 to 80 ppb and to show consistency in their individual measurements (Choinière and Barrington, 1998; Edeogn et al., 2001). In the field, the panellists were trained to evaluate the hedonic tone (HT) of the ambient air using a scale of 0 to -10, where 0 to -2 is tolerable, -2 to -4 is unpleasant, -4 to -6 is very unpleasant, -6 to -8 is terrible and -8 to -10 is intolerable. For each day of field testing, HT evaluations were translated into OC (OU m^{-3}) by asking the panellists in the laboratory, to evaluate the HT of various dilutions of the odorous air samples collected at the generator and at known OC strengths. The reading of each panellist forming a group of four was averaged to convert the field HT observations into OC.

The laboratory forced choice dynamic olfactometer used in this experiment was fully automated and capable of analyzing 4 contaminated air samples in 20 minutes, using 12 panellists. The olfactometer is unique because of its level of automation and speed suitable to evaluate air samples (Choinière and Barrington, 1998).

2.4 The field testing operation

Before each field test, the odour generator and weather station tower were checked and installed upwind from the windbreak. During the tests, the odour generator was positioned upwind from the windbreak, at a distance of 15, 30, 49 or 60 m. Each three groups of four panellists was assigned evaluation points organized in a zigzag pattern over part of a 25 ha area (500 m x 500 m downwind from the windbreak or odour generator) and given a GPS to keep track of their exact field position. Panellist paths were also designed to overlap each other.

Site 1 one row of mature poplars   Site 2 mixed mature deciduous trees

Site 3 one row of conifers   Site 4 mature conifers
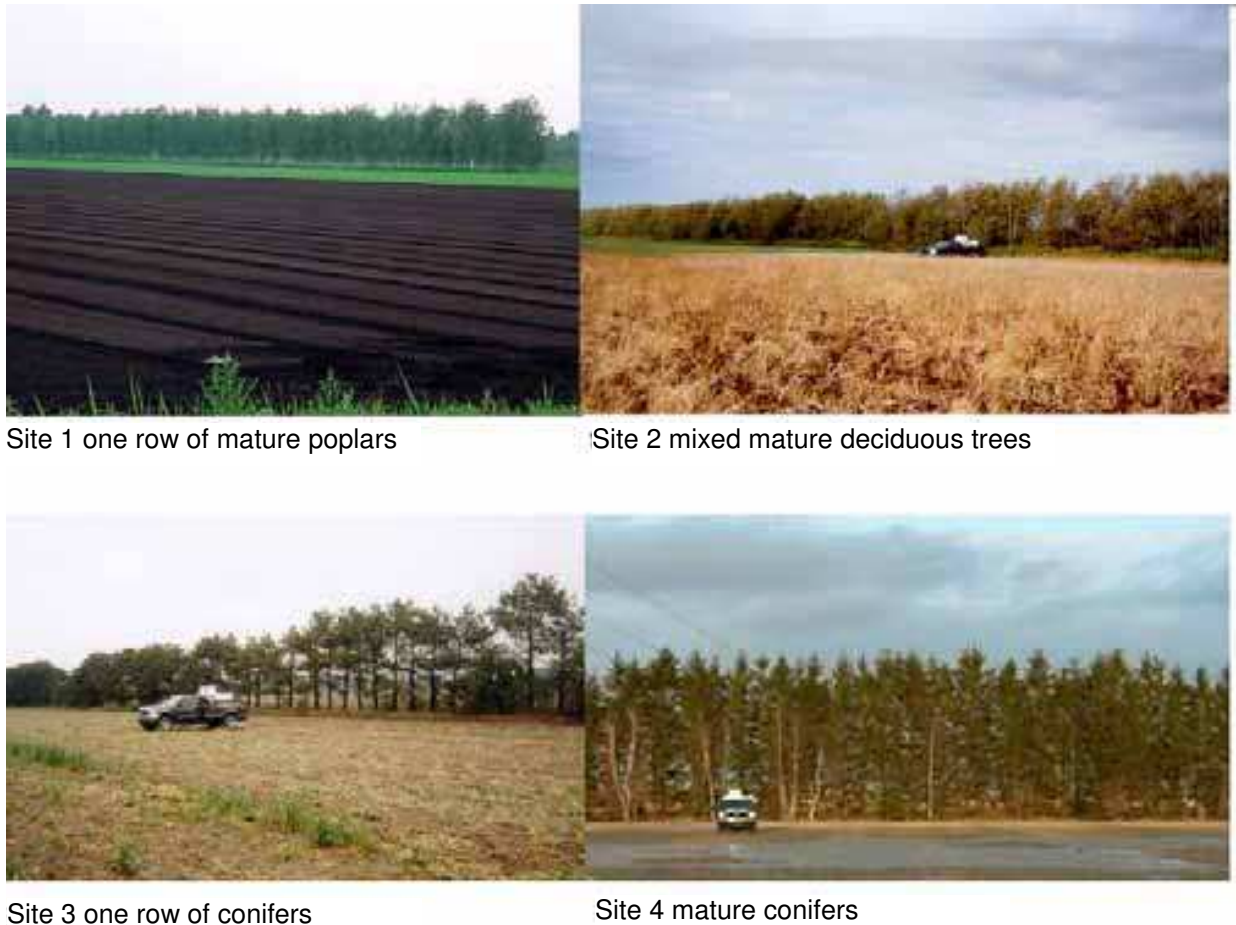
Fig. 2. The four experimental windbreaks each offering a different type of tree and/or porosity (Lin et al., 2006)

After operating the odour generator for 15 minutes, the groups of panellists would start covering their specified overlapping zigzagged path and measure the odour plume. At each measurement point, the group would stop walking, removed their face masks and evaluate for one minute the hedonic tone (HT) of the ambient air using the scale of 0 to -10. An odour point was defined as a point in the field where at least 50 % (2 out of 4) of the panellists detected an odour. The HT of the ambient air at an odour reading point was averaged from the four panellist evaluations.

During each test day, the odour plume was observed in the morning by 12 trained panellists. Then, in the afternoon, the same 12 panellists evaluated the air samples collected at the odour generator using the laboratory olfactometer. This laboratory work served two purposes: measure the odour concentration (OC in OU m^{-3}) of each odorous air sample, and; correlate the measured field hedonic tone (HT) observed by the panellists with odour concentration values. This correlation was then used to translate the HT plumes into OC plumes.

During 18 days between the end of August and the beginning of December 2003, 39 different tests were conducted on the 4 windbreak sites and the single control site (Lin et al., 2006). On the control site without a windbreak, 6 repeated tests were conducted on 4 different days. Then, 33 tests were conducted on the 4 windbreak sites. A total of 12, 11, 9 and 1 tests were conducted with the odour generator located 15, 30, 60 and 49 m upwind

from the windbreak, respectively. Tests on site 4 were conducted in December 2003, because of delays in finding a suitable windbreak site.

During each test, the odour generator emitted a decreasing odour level and, from one test to other, the odour level varied. Each odour plume was therefore standardized for purposes of comparison. Thus, the odour concentration measured at every station by each group of panellists, at a given period in time, was divided by the odour concentration of the generator at that time, and multiplied by the average odour level of 471.6 OU m^{-3} calculated from all 39 tests.

Description	Site			
	1	2	3	4
Tree type	poplar	mixed mature deciduous	conifers	conifers
Windbreak - length (m) - height (m) - depth (m) - optical porosity (fraction) - porosity at the base (fraction)	2100 18.3 0.55 0.70	1050 9.2 7 0.35 0.30	405 7.6 0.55 0.70	380 15.2 6 0.35 0.40
Location	Sherrington	St Chrysostome	St Amable	St Charles

Table 1. Description of experimental windbreak sites with tree type. All locations are located within 50km of the Island of Montreal, Canada, in the south west region

2.5 The statistical analysis of panelist performance and windbreak dispersion

In the laboratory, the panellists HT as observed in the field needed to be translated into an odour concentration value (OC) using the forced choice dynamic olfactometer. During the 39 tests conducted over 18 days, the odorous air released by the odour generator was samples 78 times or once every 30 minutes. From these 78 samples, 56 were used to have the panellists produced sets of HT and corresponding OC readings. Based on these data sets, a regression equation was produced to correlate OC with HT using SAS (SAS Institute Inc., 2001).

Based on the field data, the effect of the windbreak on the size of the odour plume was tested statistically. A 2 OU m^{-3} contour for each measured odour plume was plotted and enclosed within a rectangle to define its length and width equal to the side of the rectangle parallel and perpendicular to the average wind direction, respectively. The statistical classification and covariance models were used to analyze the various factors affecting the size of the odour plume (length and width). The covariance model is the combination of the regression and classification models in the same analysis of variance model (SAS Institute Inc., 2001). The distance between the windbreak and the odour generator (DWO), atmospheric stability (AS), and windbreak porosity were fixed factors used for the classification, and wind speed, wind angle against the windbreak (90° being perpendicular), odour emission rate (OER) and temperature (T) were the continuous factors used for the regression analysis. Tree height and type were not considered in the analysis.

3. Model development

The Computational Fluid Dynamic used for this modelling was based on the SST k-ω model capable of considering a high level of turbulence (Fluent inc., 2005). The model development respected the following steps: 1) determining the governing equations; 2) meshing the computational domain; 3) selecting the solver capable of defining the fluid properties and its components such as the windbreak, and; 4) setting boundary conditions.

3.1 Governing equations

The air flow moving from one computational cell to the next must respect the governing equations of mass, momentum, energy and species conservation expressed as:

$$\frac{\partial \rho}{\partial t} + \frac{\partial}{\partial x_i}(\rho u_i) = 0 \tag{1}$$

$$\frac{\partial}{\partial t}(\rho u_i) = -\frac{\partial}{\partial x_j}(\rho u_i u_j) - \frac{\partial p}{\partial x_i} + \frac{\partial}{\partial x_j}\left[\mu\left(\frac{\partial u_i}{\partial x_j} + \frac{\partial u_j}{\partial x_i} - \frac{2}{3}\delta_{ij}\left(\frac{\partial u_1}{\partial x_1} + \frac{\partial u_2}{\partial x_2} + \frac{\partial u_3}{\partial x_3}\right)\right)\right]$$
$$+ \frac{\partial}{\partial x_j}\left(-\rho \overline{u_i' u_j'}\right) + \rho g_i - \frac{\mu}{\alpha}u_i - \frac{1}{2}C_{ir}\rho u_{mag} u_i \tag{2}$$

$$\frac{\partial}{\partial t}(\rho E) + \frac{\partial}{\partial x_j}\left[u_j\left(\rho E + p\right)\right] = \frac{\partial}{\partial x_j}\left(k_{eff}\frac{\partial T}{\partial x_j} - \sum_i h_i J_i + u_i\left(\tau_{ij}\right)_{eff}\right) + S_h \tag{3}$$

$$\frac{\partial}{\partial t}(\rho Y_i) + \nabla \bullet (\rho u Y_i) = -\nabla \bullet J_i \tag{4}$$

where ρ is fluid density; t is time; u_i (i=1, 2, 3, indicating x, y, and z direction) is the mean velocity u in ith direction; u_i 'is the fluctuating component of the instantaneous velocity; μ is fluid viscosity; δ_{ij} is the unit tensor; p is the static pressure; g_i is the gravitational acceleration constant in the ith direction; a is the aerodynamic porosity or permeability of the windbreak; a^{-1} is the viscous resistance coefficient; C_{ir} is the inertial resistance coefficient caused by the windbreak; u_{mag} is the magnitude of the velocity (Hinge, 1975; Saatjian, 2000); E is the total energy; k_{eff} is the effective thermal conductivity; S_h represents all volumetric heat sources such as those of chemical reactions; T is temperature, and; $(\tau_{ij})_{eff}$ is the effective deviatoric stress tensor.

The coefficients Y_i, J_i and h_i are the mass fraction, diffusion flux and the sensible enthalpy of the ith atmospheric species (Bird et al., 2002; Fox & McDonald, 1992). The term $-\rho u_i$ 'u_j ' is called the Reynolds stresses.

In Eq. (4), the diffusion flux J_i of the atmospheric species i, arises due to concentration gradients. The diffusion flux for turbulent flow is:

$$J_i = -(\rho D_{i,m} + \frac{\mu_t}{Sc_t})\nabla Y_i - D_{T,i}\frac{\nabla T}{T} \tag{5}$$

where Y_i is mass fraction of the species i; $D_{i,m}$ is the diffusion coefficient for species i in the mixture; and $D_{T,i}$ is the thermal diffusion coefficient; Sc_t is the turbulent Schmidt number generally equal to 0.7, and; μ_t is the turbulent viscosity (Saatjian, 2000; Bird et al., 2002).

3.2 Describing the windbreak

A windbreak is a porous medium resisting wind or air flow and therefore constituting a momentum sink. This resistance can be introduced in the momentum equation in terms of viscous and inertial resistance:

$$F_i = -\frac{\mu}{\alpha} u_i - \frac{1}{2} C_{ir} \rho u_{mag} u_i \tag{6}$$

where F_i is the resistance to wind flow; μ is fluid viscosity; a is the aerodynamic porosity or permeability of the windbreak; a^{-1} is the viscous resistance coefficient; C_{ir} is the inertial resistance coefficient caused by the windbreak; u_{mag} is the magnitude of the average velocity, and; u_i (i=1, 2, 3, indicating x, y, and z direction) is the mean velocity u in ith direction. The term $\mu\, u_i/a$ in Eqn (6) is Darcy's law for porous medium which calculates the resistance exerted by the windbreak due to fluid viscosity (Bird et al., 2002). The term ($C_{ir}\, \rho\, u_{mag}\, u_i /2$) in Eqn (6) computes the inertial loss of the fluid flowing through the windbreak, which varies over the height of the tree depending on its shape (Wang & Takle, 1995; Wilson, 2004; Wilson, 1985). Poplars offer dense foliage at their top compared to conifers which offer more foliage at their base. Accordingly, a valid simulation uses an inertial resistance coefficient which varies over tree height.

In this project, the simulated windbreak was designed as a cubic volume with a specific width, height, length and optical porosity, positioned at a specific distanced x downwind from the odour source. The optical porosity was used to compute the aerodynamic porosity representing the exact amount of air flowing through the foliage of the windbreak. The aerodynamic porosity, or permeability, is defined as the ratio of wind speed perpendicular to the windbreak, immediately downwind and averaged over the full height of the windbreak, to that upwind from the windbreak (Guan et al., 2003; Wang & Takle, 1995):

$$\alpha = \frac{\int_{0@windbreak}^{H} u_1 dz}{\int_{0@inlet}^{H} u_1 dz} \tag{7}$$

The relationship between optical and aerodynamic porosity is defined according to the wind tunnel measurements of Guan et al. (2003):

$$\alpha = \beta^{0.4} \tag{8}$$

where α is the aerodynamic porosity and β is the optical porosity. Accordingly, an optical porosity of 0.35 results in an aerodynamic porosity of 0.66, implying that 66 % and 34 % of the air flows through and over the windbreak, respectively.

To calibrate and validate the model, the field work in this project observed the effect of tree types (poplar and deciduous, Fig. 3) and size forming the windbreaks using sites 1, 2 and 3 (Table 1). On site 1, the windbreak consisted of mature deciduous trees offering an averaged optical porosity of 0.35 but the optical porosity at its base was 0.30 while that over the rest of its profile was 0.40. Therefore, the inertial resistance C_{ir} was defined as proportional to the density (1.0 minus its porosity) of the windbreak:

$$C_{ir} = \begin{cases} w_1 - \dfrac{w_1 - w_2}{h_1} z & z \le h_1 \\ w_2 - \dfrac{w_2 - w_3}{H - h_1}(z - h_1) & h_1 < z \le H \end{cases} \tag{9}$$

(a)   (b)
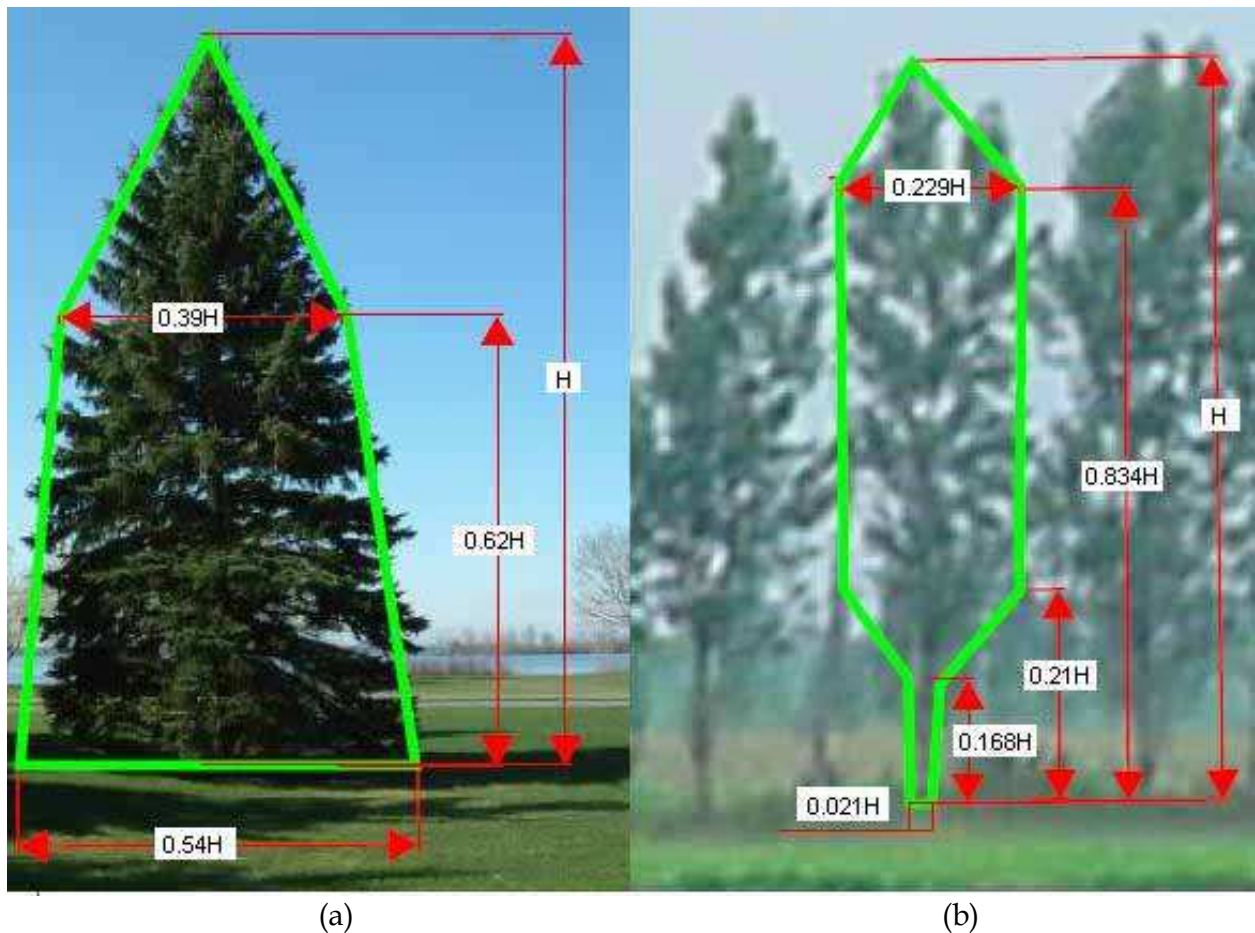
Fig. 3. The structure of the trees forming the windbreak, where H is the total height;
a) conifer; b) poplar (Lin et al., 2007b)

where z is the coordinate value in the vertical direction; H is the height of the windbreak; h_1 is the height at which the porosity of the windbreak changes ($0 < h_1 < H$), and; w_1, w_2, and w_3 are three constants corresponding to the thickness of the real windbreak, set in the simulation to allow 66 % of the air to pass through.

For the windbreak on site 2, the averaged optical porosity was 0.35: the optical porosity at the base was 0.40; that between heights of 3 to 14 m was 0.3, and; above 14 m, the porosity was gradually increased from 0.3 to 1.0. Therefore C_{ir} was:

$$C_{ir} = \begin{cases} w_1 - \dfrac{w_1 - w_2}{h_1} z & z \le h_1 \\ w_2 & h_1 < z \le h_2 \\ w_2 - \dfrac{w_2 - w_3}{H - h_2}(z - h_2) & h_2 < z \le H \end{cases} \tag{10}$$

where w_1, w_2, and w_3 were set at 0.27, 0.39 and 0.05, and; h_1, h_2 and H were set at 3, 14 and 15 m, respectively. Again, such conditions allowed 66 % of the air to pass through the windbreak. The windbreak on site 3 offered an average optical porosity of 0.55. Its porosity was assumed to be 0.7 at a height of 1.0 m, to linearly decrease to 0.47 at a height of 3 m, to remain constant between the height of 3 to 15 m, and; then, to increase to 1.0 at the tree top. These conditions produced an average air permeability of 0.79 and a C_{ir} calculated as:

$$C_{ir} = \begin{cases} w_1 & z \leq h_1 \\ w_1 + \dfrac{w_2 - w_1}{h_2 - h_1}(z - h_1) & h_1 < z \leq h_2 \\ w_2 & h_2 < z \leq h_3 \\ w_2 - \dfrac{w_2}{H - h_3}(z - h_3) & h_3 < z \leq H \end{cases} \tag{11}$$

where w_1 and w_2 were set at 0.1 and 0.205, and; h_1, h_2, h_3 and H were set at 1, 3, 15 and 18 m, respectively.

3.3 Computational domain

The computational domain was designed as a volume measuring 690 m in length (75 H, H being the height of the windbreak of 9.2 m), 184 m (20 H) in width and 73.6 m (8 H) in height (Fig. 4). The left and right faces of the space were the wind inlet and outlet, located 138 and 552 m from the origin, respectively. The front, back and top faces of the volume were set to have an open or undisturbed wind velocity and were positioned at 92, -92 and 73.6 m from the origin, respectively. The bottom face of the volume was the ground surface.

The odorous air was introduced into this computational volume by a single source opening measuring 1.5 m × 0.376 m × 1.75 m in x, y, z directions with the right face positioned at x = 0 m and the front face at y = -0.188 m. The centre of the odour emission surface was positioned at x = 0 m, y = 0 m and z = 1.562 m. Odours were blown from the right-up rectangular face (the red zone in Fig. 4) measuring 0.376 × 0.376 m. The windbreak (green zone in Fig. 4) was designed as a porous cubic volume.

For computational purposes, the computational volume was meshed into 228, 81, and 46 segments in the x, y and z coordinates, respectively, and the size of the rectangular cells gradually increased from the odour generator towards the outward faces of the system. For the odour inlet, 64 rectangles were meshed over an area of 0.376 × 0.376 m² to effectively transfer the odour mass fraction to other cells.

3.4 Numerical solver

The Reynolds stresses in Eq. (8) can be computed using the Boussinesq Hypothesis based on the mean velocity gradients:

$$-\rho \overline{u_i' u_j'} = \mu_t \left(\frac{\partial u_i}{\partial x_j} + \frac{\partial u_j}{\partial x_i} \right) - \frac{2}{3}\left(\rho k + \mu_t \frac{\partial u_i}{\partial x_i} \right)\delta_{ij} \tag{12}$$

where μ_t is the turbulent viscosity, and; k is the turbulence kinetic energy.

Selected to perform the simulations, the SST k-ω model of the Fluent software uses two different transport equation to express the turbulence kinetic energy k and the specific

dissipation rate ω. The SST k-ω accounts for the principal turbulent shear stress and uses a cross-diffusion term in the ω equation to blend both the k-ω and k-ε models and to ensure that the model equations behave appropriately in both the near-wall and far-field zones. Thus, the SST k-ω model offers a superior simulation performance as compared to the individual k-ω and k-ε models (Menter et al., 2003).

The Fluent 6.2 steady 3-dimension segregated solver was used to solve the SST k-ω model through second and quick orders of discretisation schemes converting the governing equations into algebraic equations solved numerically while increasing the calculation accuracy. The second order scheme was used to compute the pressure, the second order upwind scheme was used to compute odour dispersion and the quick scheme was used to compute momentum, turbulence kinetic energy, turbulence dissipation rate and energy. The SIMPLE method was applied to the velocity and pressure coupling (Fluent inc., 2005).

3.5 Fluid properties

Livestock manures emit over 168 odorous compounds and six of the ten compounds with the lowest detection thresholds contained sulphur (O'Neil & Phillips, 1992). Hydrogen sulphide (H_2S) was selected as odour and presumed to flow along with clean dry air. Therefore, the modelled fluid was defined as clean air and H_2S and its mass fraction at the odour source was:

$$Y_2 = \frac{OC_g \bullet m_{H_2S}}{\dfrac{P_a M_1}{RT} + OC_g \bullet m_{H_2S}} \tag{13}$$

where Y_2 is the odour mass fraction (OMF) at the odour inlet, or the ratio of the odour mass to the total air and odour mass in 1.0 m^3, dimensionless; P_a is the atmospheric pressure of 101325 Pa at sea level; T is temperature in K; M is the molecular weight of dry air or 0.028966 kg mol^{-1}; R is the universal gas constant or 8.31432J mol^{-1} K^{-1} (ASHRAE, 2009); OC_g is the odour source concentration, in OU m^{-3}, and; m_{H2S} is the mass of H_2S required to produce one odour unit, expressed as kg OU^{-1} and $m_{H2S} = 7.0 \times 10^{-9}$ kg OU^{-1} (Blackadar, 1997).

Description	Unit	Mixture	Air	H_2S
Density	kg m^{-3}	Impressible-ideal-gas law		
Cp	J kg^{-1} K^{-1}	Mixing law	1005.422	1005.333
Thermal conductivity	W m^{-1} K^{-1}	Mass-weighted-mixing-law	0.0260411	0.0137023
Viscosity	kg m^{-1} s^{-1}	Mass-weighted-mixing-law	1.458E-6 $T^{1.5}$ / (T + 110.1)	-1.4839E-6 + 5.1E-8T -1.26E-11 T^2
Mass diffusivity	m^2 s^{-1}	-1.3497E-5 + 1.05772E-7T		
Thermal diffusivity coefficient	kg m^{-1} s^{-1}	Kinetic-theory		
Molecular weight	kg $kgmol^{-1}$		28.966	34.07994

Table 2. Properties of clean air and H_2S used in the simulation where T is temperature in K, and for a temperature range of 283 to 313 K

The modelled fluid was defined using the physical properties of clean dry air and H2S, including density, specific heat capacity, thermal conductivity, viscosity, mass and thermal diffusion coefficients for the mixture and individual species. The modelled fluid was considered incompressible and its density varied with temperature but not with pressure because of a Mach number under 10 %. The fluid's specific heat capacity, thermal conductivity and viscosity were calculated using the mass mixing-law and the thermal diffusion coefficient was calculated using the kinetic-theory (Table 2).
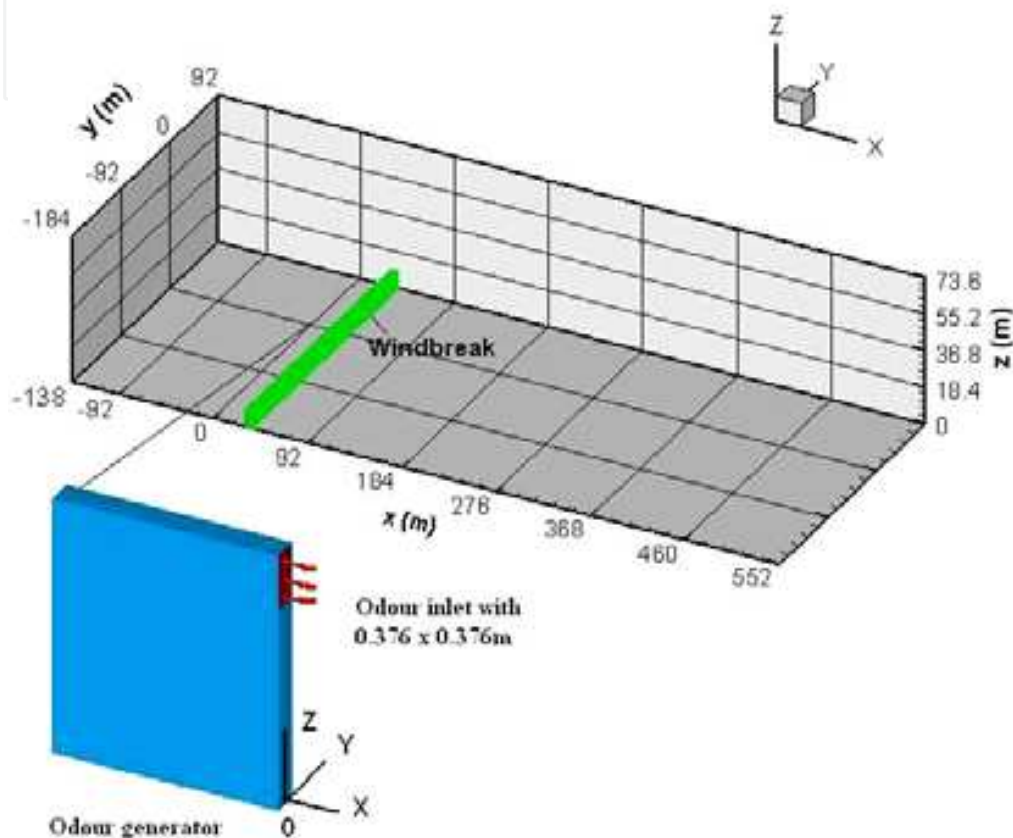
Fig. 4. The computational volume schematics used to predict odour dispersion. In this case, the z coordinate is magnified 2 times and the windbreak optical porosity is 0.35. The green bar represents the windbreak and the odour emission surface centre of the odour generator is located at x = 0, y = 0 and z = 1.562 m

3.6 Boundary conditions
The boundary conditions define the faces of the computational volume and the velocity inlet of the clean air and odorous gas. The bottom face of the odour dispersion system (ODS) was assumed to be no slip requiring as input only temperature and roughness length. As air inlet velocity, the inputs included the vertical profile of the horizontal wind velocity, temperature, turbulence kinetic energy and specific dissipation rate.

The odour dispersion around the windbreak was assumed to occur in the homogeneous plat terrain of the surface layer of the atmosphere, and the approaching wind flow was assumed not to change the vertical direction of horizontal velocity and to satisfy the assumption of the Monin Obukhov similarity theory. Atmospheric stability was determined by the Monin Obukhov length L_{MO}:

$$L_{MO} = -\frac{u_*^3 \rho C_p T}{k_a g H_F} \tag{14}$$

where u_* is the friction velocity; k_a is the von Karman constant ranging from 0.35 to 0.43 and usually equal to 0.4; T is the surface temperature; C_p is the specific heat of air; H_F is the vertical heat flux; ρ the air density, and; g is the gravitational acceleration constant (Schnelle, 2000). When the convective heat flux is upward, L_{MO} is negative and the air is unstable. When the earth absorbs heat energy, the heat flux is negative, L_{MO} is positive and hence the air is stable. However, when the heat flux is zero, L_{MO} is infinite and the air stability conditions are neutral.

The vertical profile of the horizontal mean wind velocity is calculated by:

$$u_{mag}(z) = \begin{cases} \dfrac{u_*}{k_a} \ln \dfrac{z}{z_0} & h_{ABL}/L_{MO} = 0 \quad \textit{neutral} \\[3mm] \dfrac{u_*}{k_a}\left(\ln \dfrac{z}{z_0} - \ln \dfrac{(1+x)^2(1+x^2)}{(1+x_0)^2(1+x_0^2)} + 2\tan^{-1}(x) - 2\tan^{-1}(x_0) \right) & h_{ABL}/L_{MO} < 0 \quad \textit{unstable} \\[3mm] \dfrac{u_*}{k_a}\left(\ln \dfrac{z}{z_0} + \dfrac{5(z-z_0)}{L_{MO}} \right) & h_{ABL}/L_{MO} > 0 \quad \textit{stable} \end{cases} \tag{15}$$

where

$$x = \left(1 - \frac{16z}{L_{MO}} \right)^{\frac{1}{4}} \tag{16}$$

$$x_0 = \left(1 - \frac{16z_0}{L_{MO}} \right)^{\frac{1}{4}} \tag{17}$$

where u_{mag} is the magnitude of the horizontal mean wind velocity at height z above the surface ($z \geq z_0$); z_0 is the roughness length of the surface, h_{ABL} is the height of the atmospheric boundary layer, and L_{MO} is the Monin Obukhov length (Panofsky & Dutton, 1984; Blackadar, 1997; Jacobson, 1999).

Assuming that the potential temperature is equal to the temperature at z_s, the vertical temperature profile $T_{(z)}$ can be calculated as (Panofsky & Dutton, 1984):

$$T(z) = \begin{cases} -\gamma_d(z-z_s) + T & h_{ABL}/L_{MO} = 0 \quad \textit{neutral} \\[3mm] -\gamma_d(z-z_s) + T_s\left(1 + \dfrac{u_*^2}{\kappa_a^2 g L_{MO}}\left(\ln \dfrac{z}{z_s} - 2\ln \dfrac{1 + \sqrt{1 - \dfrac{16z}{L_{MO}}}}{1 + \sqrt{1 - \dfrac{16z_s}{L_{MO}}}} \right) \right) & h_{ABL}/L_{MO} < 0 \quad \textit{unstable} \\[3mm] -\gamma_d(z-z_s) + T_s\left(1 + \dfrac{u_*^2}{\kappa_a^2 g L_{MO}}\left(\ln \dfrac{z}{z_s} + \dfrac{5(z-z_s)}{L_{MO}} \right) \right) & h_{ABL}/L_{MO} > 0 \quad \textit{stable} \end{cases} \tag{18}$$

where z_s is a height of 1.35 m above ground; T_s is the temperature at height z_s; g is the gravitational acceleration constant, and; Y_d is the dry adiabatic lapse rate of 0.01 K m^{-1}.

The vertical turbulence kinetic energy profile within the surface atmospheric layer can be defined as:

$$k(z) = \frac{1}{2}\left(\sigma_u^2 + \sigma_v^2 + \sigma_u^2\right) \tag{19}$$

where $k(z)$ is the turbulence kinetic energy (TKE), and; σ_u, σ_v and σ_w are turbulence components in the x, y, z coordinates.

For neutral conditions, $h_{ABL}/L_{MO} = 0$, TKE linearly decreased with height, and at the top of the atmospheric boundary layer, equals 20 % of its value at the ground level (Carruthers & Dyster, 2006). The TKE for neutral condition is:

$$k(z) = 5.97u_*^2 T_{WN}^2 \tag{20}$$

where

$$T_{WN} = 1 - a_s \frac{z - z_0}{h_{ABL} - z_0} \tag{21}$$

where $a_s = 0.8$.

For unstable conditions ($h_{ABL}/L_{MO} < 0$), the TKE is:

$$k(z) = 5.97u_*^2 T_{WN}^2 + w_*^2\left(0.3 + 0.2T_{WC}^2\right) \tag{22}$$

where

$$T_{WC} = 2.1\left(\frac{z - z_0}{h_{PBL} - z_0}\right)^{\frac{1}{3}} T_{WN} \tag{23}$$

$$w_* = u_*\left(\frac{h_{ABL} - z_0}{k_a|L_{MO}|}\right)^{\frac{1}{3}} \tag{24}$$

where w_* is the mixing layer velocity scale.

For stable conditions ($h_{ABL}/L_{MO} > 0$), TKE is expressed as:

$$k(z) = 5.97u_*^2 T_{WN}^{\frac{3}{2}} \tag{25}$$

and $a_s = 0.5$ for roughness length $z_0 \geq 0.1$ m.

The vertical turbulence specific dissipation rate $\omega(z)$ is:

$$\omega(z) = \frac{k(z)^{\frac{1}{2}}}{0.09^{\frac{1}{4}}l} \tag{26}$$

where l is the turbulence length scale set as twice the height of the ground surface roughness length ($2z_0$) based on a calibration of the horizontal velocity recovery rate downwind from the windbreak (Schnelle, 2000; Menter, 2003).

The parameters defining the surface layer conditions in the SST model, namely z_0, L_{MO}, h_{ABL}, u_* and T_s are determined according to the simulation conditions. Corresponding to the physical conditions of the ground surface, z_0 was 0.13 m (Lin et al., 2007b). The coefficient L_{MO} was estimated from the Pasquill atmospheric stability categories. When z_0 was 0.13 m, the average L_{MO} was -20 m for the Pasquill stability category B, and was 20 for the stability category F (Golder, 1972). The coefficient h_{ABL} was designated as the average rural mixing height for each stability category measured at the weather station. Once z_0, L_{MO} and h_{ABL} were determined, u_* and T_s were calculated from the temperature and wind velocity measured at a height of 10 m and using Eqs. (15) and (18), respectively.

3.7 Simulating the effect of weather conditions

The effect on odour plume length of climatic factors was tested through 21 simulations (Table 3): simulations 1 to 9 for wind velocity; simulations 10 to 12 for air temperature; simulations 13 to 19 for wind direction, and; simulations 20 and 21 for atmospheric stability. Simulations 1 to 12, 20 and 21 respected an odour dispersion system (ODS) as shown in Fig. 4, and presumed a constant odour concentration at the source of 300 OU m^{-3}. For simulations 13 to 19, the ODS measured 460 m × 414 m × 73.6 m, and the odour concentration at the source was 550 OU m^{-3}. For all simulations, the surface roughness length was 0.13 m, the odour generator emitted odorous air at a rate of 1.6 m^3 s^{-1} and the natural windbreak consisted of a single row of conifers, measuring 7.0 m in width and 9.2 m in height and offering an aerodynamic porosity of 0.4 with a coefficient C_{ir0} equal to 0.08706. The windbreak was located 30 m downwind from the odour source.

Simulations 1 to 9 tested the effect on odour dispersion of the wind velocity for unstable (category B), neutral (category D) and stable (category F) atmospheric conditions for their average T, L_{MO} and h_{ABL} values. The wind velocity ranges were measured in September 2003 at PE Tudeau airport by Environment Canada for stability category B, D and F. For simulations 1, 2 and 3 under stability category B, the averaged values of T, L_{MO} and h_{ABL} were 293 K, -20 m and 1390 m and the velocities were 1.0, 1.8 and 3.0 m s^{-1}, respectively (Table 8.2). For simulations 4, 5 and 6 under stability category D, the averaged T, L_{MO} and h_{ABL} were 291 K, infinity (∞) and 2090 m, and the velocities were 3.0, 5.4 and 6.4 m s^{-1}, respectively. Finally, for simulations 7, 8 and 9 under stability category F, the averaged T, L_{MO} and h_{ABL} were 287 K, 20 m and 1811 m, and the velocities were set at 1.0, 1.9 and 3.0 m s^{-1}, respectively.

Temperature effects were tested under unstable, neutral and stable atmospheric stability categories, using simulations 10, 11 and 12 with average December 2003 temperatures of 269, 270 and 265 K, and simulations 2, 5 and 8 with average September temperature of 293, 291 and 287 K.

Simulations 13 to 19 tested the effect of the wind direction, measured from the positive x-axis and set at 0, -15, -30, -45, -60, -75 and -90°, respectively. The weather atmospheric stability category D was assumed and T, L_{MO}, h_{ABL} and wind velocity were 291 K, ∞, 2090 m and 5.4 m s^{-1}, respectively.

The effect of the atmospheric stability was tested twice. Simulations 2, 5 and 8 compared average values of wind velocity, atmospheric boundary layer height and temperature. Simulations 4, 20 and 21 were also similar except for their respective stability categories B, D and F. For these three simulations, wind velocity, h_{ABL} and T were set at 3.0 m s^{-1}, 2090 m and 291 K, respectively, which are mean values for the atmospheric stability categories B, D and F.

Test	Weather condition						Computed results				
	u_{mag} at 10 m	T at 10 m	Wind	Atm. Stab.	L_{MO}	h_{ABL}	Length 1	Length 2	Length 3	Width	Height
Unit	m s⁻¹	°K	°	A-F	m	m	m	m	m	m	m
1	1	293	0	B	-20	1390	394	353	323	48	67
2	1.8	293	0	B	-20	1390	>552	465	404	48	41
3	3	293	0	B	-20	1390	>552	397	268	38	17
4	3	291	0	D	infinite	2090	>552	395	271	47	18
5	5.4	291	0	D	infinite	2090	444	235	170	34	16
6	6.4	291	0	D	infinite	2090	379	205	151	32	18
7	1	287	0	F	20	1811	>552	>552	552	48	25
8	1.9	287	0	F	20	1811	>552	474	349	46	19
9	3	287	0	F	20	1811	>552	343	253	10	17
10	1.8	269	0	B	-20	1390	>552	463	404	44	41
11	5.4	270	0	D	infinite	2090	443	235	170	34	16
12	1.9	265	0	F	20	1811	>552	475	351	44	19
13	5.4	291	0	D	infinite	2090	301	168	129	31	15
14	5.4	291	-15	D	infinite	2090	231	135	102	60	15
15	5.4	291	-30	D	infinite	2090	198	117	77	67	15
16	5.4	291	-45	D	infinite	2090	187	103	92	74	15
17	5.4	291	-60	D	infinite	2090	248	150	118	40	15
18	5.4	291	-75	D	infinite	2090	342	219	180	24	15
19	5.4	291	-90	D	infinite	2090	>322	>322	301	18	11
20	3	291	0	B	-20	2090	>552	394	266	39	19
21	3	291	0	F	20	2090	>552	344	251	39	17

Table 3. Simulation test plan for weather conditions and computed results : Length 1 for the length of the odour plume for the 1 OU m⁻³, Length 2 for the 2 OU m⁻³, and Length 3 for the 3 OU m⁻³

3.8 Generating the simulated odour plumes

An odour plume is expressed by a series of odour concentration (OC) contours within a plane. In the field and at various locations, the trained panellists detected the odour hedonic tone (HT) which is the degree of pleasant or unpleasant smells, expressed using a scale 0 to -10, where 0 is neutral and -10 is extremely unpleasant (Lin et al., 2007b). In the laboratory, the panellists were then asked to detect the HT and OC of 56 odour samples, which produced the following correlation:

$$OC = \begin{cases} 0 & AHT = 0 \\ 1.3e^{0.45\,AHT} & 1 \le AHT \le 10 \end{cases} \qquad (27)$$

where OC is odour concentration in OU m⁻³, and; AHT is an absolute value of HT ranging from 0 to 10. From Eq. (27), the maximum AHT is 10 and the corresponding OC is 117 OU m⁻³. Hence, when OC exceeds 117 OU m⁻³, AHT is still defined as 10, because panellists still feel an extremely unpleasant odour.

To plot the odour plume reflecting HT, the computed dimensionless odour mass fraction (OMF) for all point of the ODS needs to be transformed into a simulated odour mass concentration (SOMC):

$$SOMC = \frac{OMF}{\dfrac{Y_2}{OC_g}} m_{H_2S} \times 10^9 \qquad (28)$$

where SOMC is simulated odour (H₂S) mass concentration in µg m⁻³; OMF is the odour (H₂S) mass fraction computed by the model for a given point in space, dimensionless; Y_2 and OC_g are the odour mass fraction and odour concentration at the odour source as defined by Eq. (28), which are respectively dimensionless and in OU m⁻³, and; m_{H_2S} is the mass of H₂S required to produce 1.0 OU m⁻³ in kg OU⁻¹ as described by Eq. (28).

Secondly, the SOMC were transformed into SAHT by correlating the 5 field test AHT (absolute HT readings) with SOMC:

$$SAHT = \begin{cases} 0.57\,SOMC^{0.46} & SOMC \le 506.5 \;\; \mu g\,m^{-3} \\ 10 & SOMC > 506.5 \;\; \mu g\,m^{-3} \end{cases} \qquad (29)$$

where SAHT is simulated absolute hedonic tone, and; SOMC is defined by Eq. (29). The field test correlation indicated a statistically significance (P < 0.01) relationship between AHT and SOMC (Lin et al., 2007b). In this procedure, the odour mass fraction of 506.5 µg m⁻³ results in AHT of 10 for an OC of 117 OU m⁻³.

4. Results and discussion

The following sections will start by characterizing the panellists, on which all results where based, and then providing a comparison for windbreak performance as observed from the field data. The modelling section will follow, starting with the model calibration using literature data, and then model application to identify the windbreak characteristics having the most influence on odour plume length, followed by the effect of climate. In all results presented, the length of the odour zone or plume is measured from the odour source. Furthermore, the strength of the odour was standardized using an average odour source emission of 471.6 OU m⁻³; this standardization compensated for the variability in odour generation between field tests.

4.1 Odour interpretation

The relationship between hedonic tone (HT) and odour concentration (OC) for the 56 samples measured during the field tests is presented in Figure 5. Collected in the morning during the odour plume observation, the field odour samples produced by the odour

generator were evaluated for their threshold dilution and hedonic tone by the same 12 panellists in the afternoon using the olfactometer. There was a dual purpose to this exercise: evaluate the odour concentration (OC) of the sample collected at the odour generator, and; obtain a correlation between odour concentrations (OC) in OU m^{-3} and hedonic tones (HT) measured in the field while sizing the odour plume.

Several interesting aspects can be concluded from Fig. 5: correlation between the odour concentration (OC) and the hedonic tone (scale of 0 to -10) is quite variable although typical of panellist response (Edeogn et al., 2001); the present panellist response differs from that of Lim et al. (2001) and Nimmermark (2006), despite the n-butanol rating of all panellists before hand, according to standards (ECN, 2001; ASTM 1997a, b).This difference resulted from culture, tolerance, and previous historical exposure to odorous situations, and; above the observed OC of 117 OU m^{-3}, the response in HT reached its peak value of -10, explaining the larger variability in reported OC value.

4.2 Field windbreak odour dispersion

The odour plumes observed in the field are far from being regular, as illustrated by Fig. 6, rather the odour plumes are formed of odour puffs resulting from the oscillating wind speed and direction. Nevertheless in terms of modelling, it will be assumed that the OC profile parallel to wind direction follows an average trend.
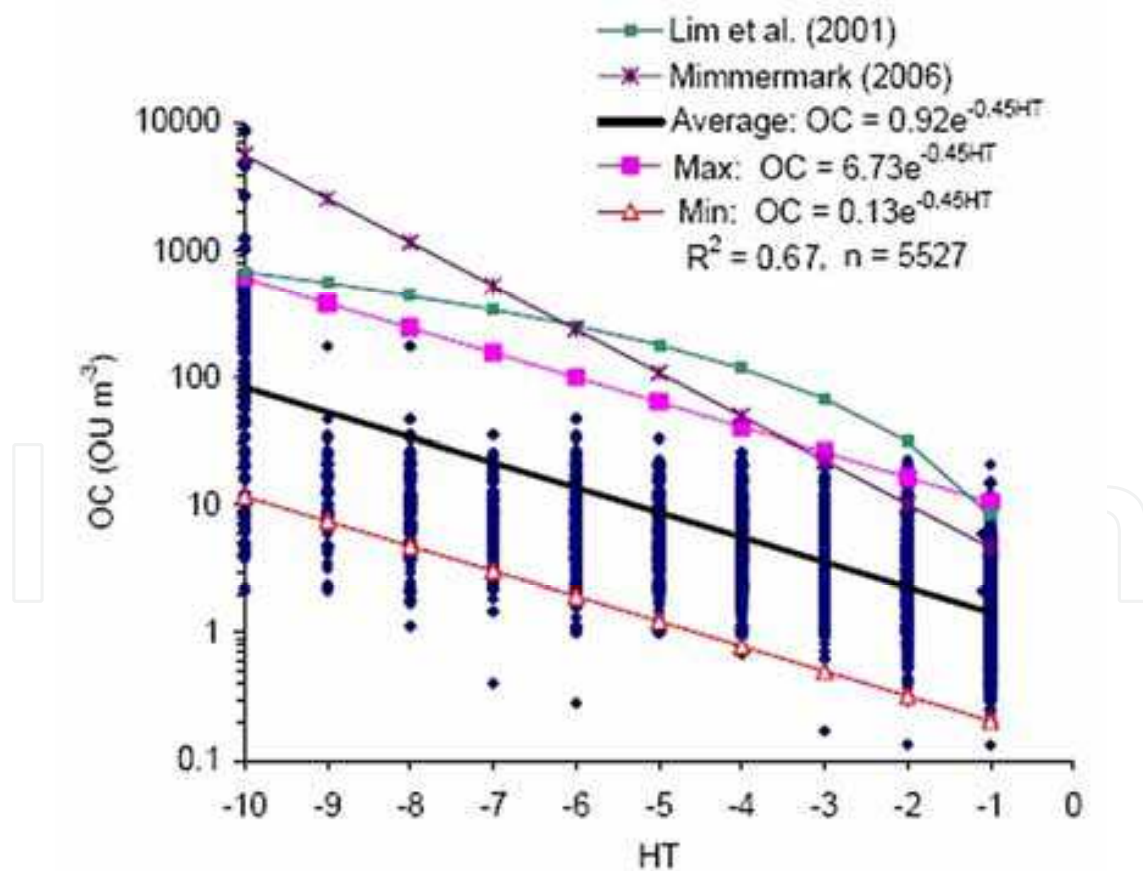
Fig. 5. Compared to data collected by Lim et al. (2001) and Nimmermark (2006), typical relationship between hedonic tone (HT) and odour concentration (OC) for the 56 air sample (minimum, average and maximum) curves (Lin et al., 2007b)

The control without a windbreak (field tests 37, 38 and 39 on site 5) is compared (Fig. 6a) to that of site 2 with a mature deciduous windbreak (field tests 5, 8, 12 and 16, on site 2) and the odour generator located 30 m upwind (Fig. 6b). The average air temperature was 26.4 and 22.6°C, respectively, for the control and windbreak sites. On site 2, the wind direction ranged between 20 to 90° with respect to the windbreak, 90° being perpendicular. Both odour plumes were observed in late August and early September under similar landscape and weather conditions.
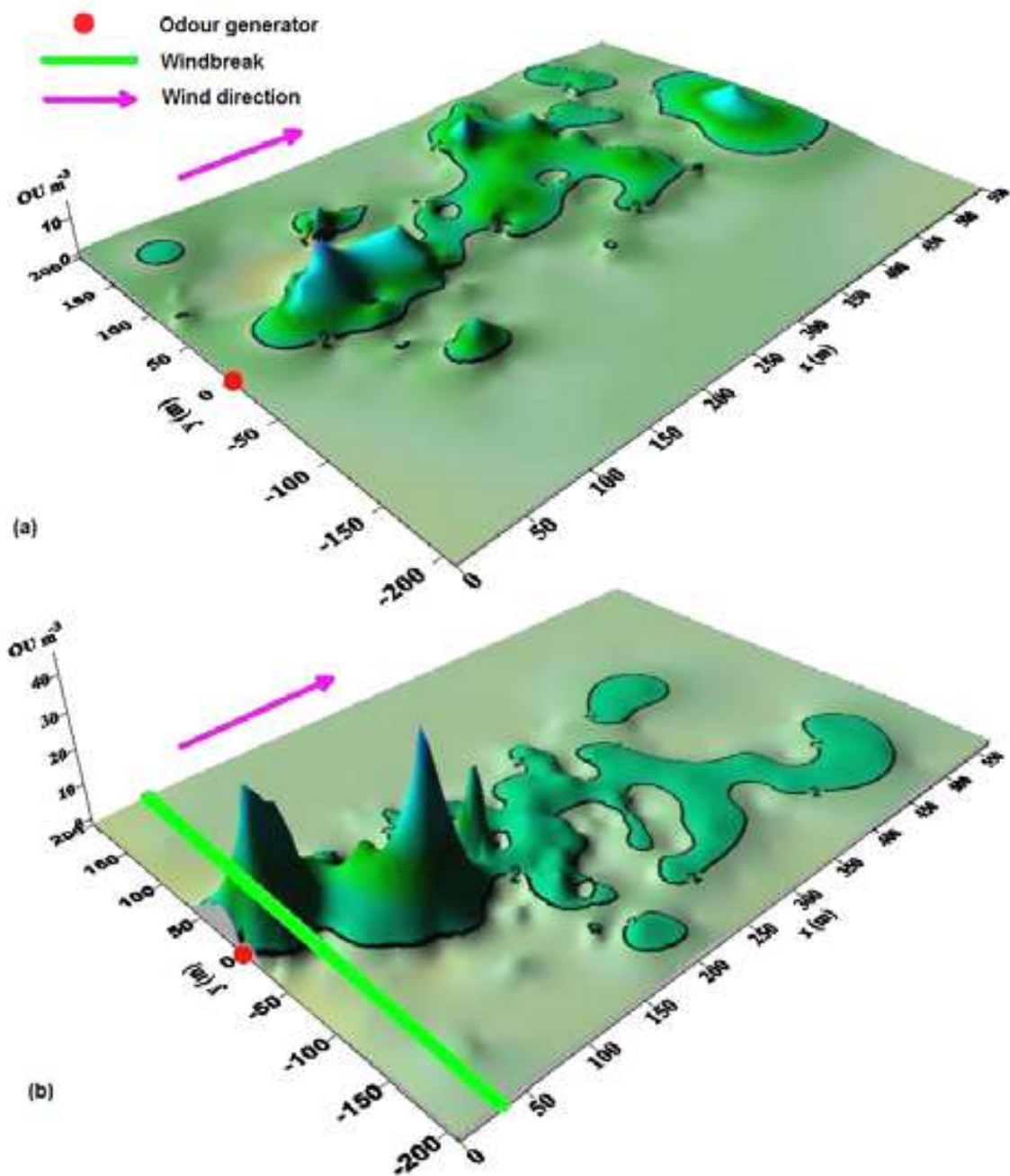
Fig. 6. Odour plumes on field sites 2 and 5 with and without a windbreak. (a) without a windbreak (tests 37, 38 and 39); (b) with windbreak on the site 2 (tests 5, 8, 12 and 16). An odour concentration of 2 OU m^{-3} is used to draw the final contour of the odorous zones (Lin et al., 2006)

Fig. 6 demonstrates that the plume developed without a windbreak reached a much longer distance downwind, compared to that developed with the windbreak. Measured furthest away, the windbreak created an odour zone of 2.0 OU m^{-3} ending at 500 m away from the source, compared to the same level of odour extending beyond 550 m for the control site. Without a windbreak, the control produced an odour plume with a maximum odour peak of 16 OU m^{-3} at a distance of 69 m while the windbreak produced a plume with a peak of 50 OU m^{-3} at a distance of 117 m. Accordingly, the windbreak is observed to concentrate or trap the odours on its leeward position before further dispersion.

The most significant parameter affecting the length of the odour plume was found to be the foliage porosity (Fig. 7). Despite the greater tree height on site 1, the more open foliage (optical porosity of 0.55) produce a longer odour plume covering 150 m in width by 600 m in length, compared to that of the windbreak on site 2 with a porosity of 0.35, generally covering a width of also 150 m but a shorter length of 300 m.
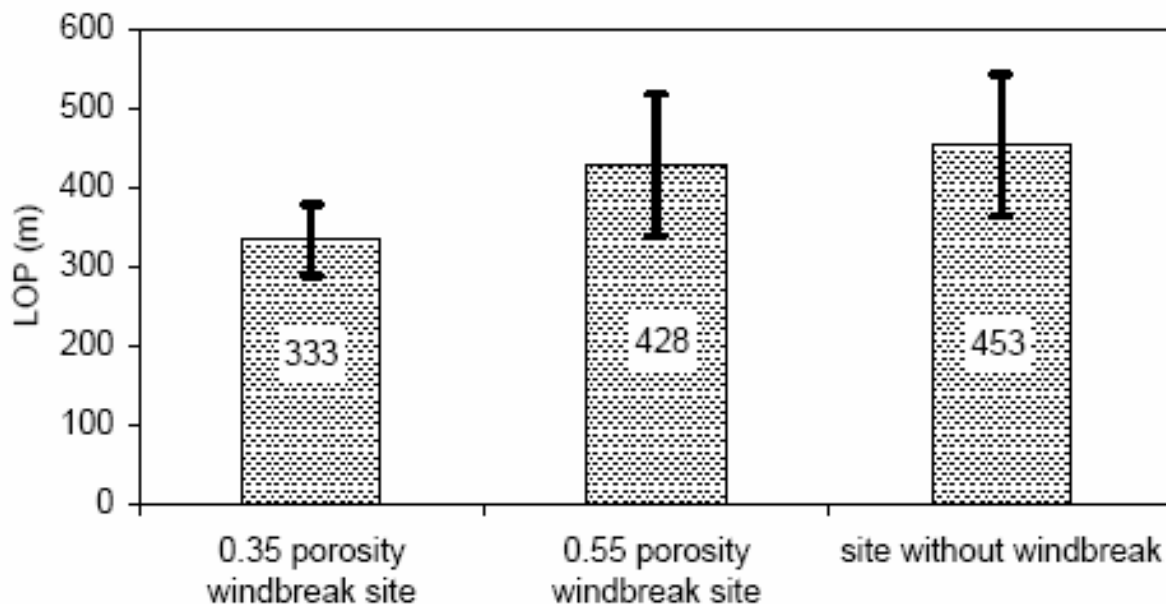
Fig. 7. The mean length of the odour plume (LOP) for the 4 field sites with a windbreak and the single control site without a windbreak; the error bars illustrates the standard error of ± 1.96 meter (Lin et al., 2007c)

The furthest measured odour concentrations for the windbreak optical porosity of 0.55 and 0.35 had values of 3.2 and 4.0 OU m^{-3} at a respective distance of 601 and 281 m. However, the windbreak optical porosity of 0.55 produced a maximum odour peak of 22 OU m^{-3} at a distance of 138 m while that with an optical porosity of 0.35 produced a maximum odour peak of 50 OU m^{-3} at a distance of 117 m. Again, the smaller odour plume corresponded to a more intense odour trapping in the leeward position of the windbreak.

In summary and for the field observation, the more open windbreak produce an odour plume similar to that of the control without a windbreak, likely because a porous windbreak produces less turbulent energy and therefore less odour mixing and odour dilution, compared to a denser windbreak. The denser windbreak with a foliage porosity of 0.35 was

able to reduce the length of the odour plume by 25 %, as compared to no windbreak, but the peak odour concentration was several times higher immediately downwind from the windbreak.

4.3 Calibrating the dispersion model

For the model to reproduce adequate wind velocities about windbreaks, the standard k-ε model was calibrated using field data measured at half height around a natural windbreak 2.2 m tall and offering an optical porosity of 0.55 (Eimern et al., 1964). The model parameter C_μ (a constant use to quantify the level of turbulent viscosity μ_t) and $C_{2\varepsilon}$ (a constant used to define the turbulent dissipation rate w) were adjusted from the default of 0.09 and 1.92, to 0.12 and 2.2, respectively. Also, the inertial resistance parameter of the windbreak was set at 10.3 m^{-1}. Once calibrated, the differences between the simulated and measured wind speeds were (Fig. 8): from -10 to 0H, lower by 4.5 %; from 0 to 30H, slightly greater by 0 to 10 %, and; at 30 H, negligible. An R^2 value of 0.97 was obtained between the measured and simulated velocity values from -10 to 30 H.
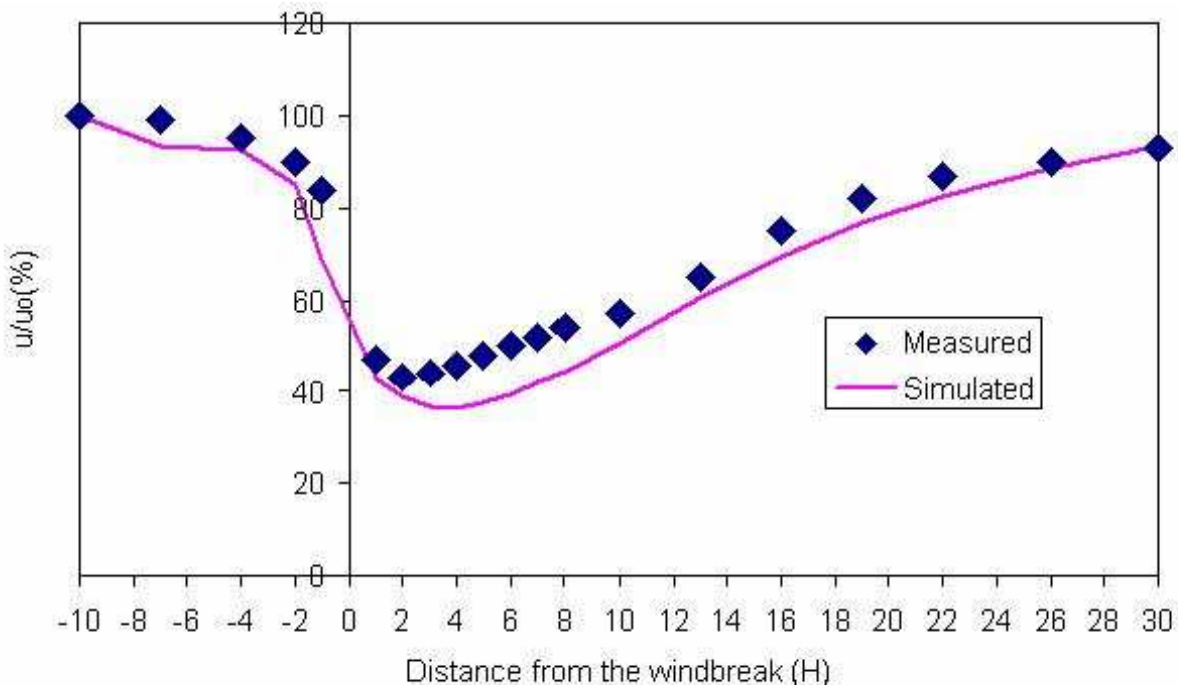
Fig. 8. Comparison of the simulated and measured wind speeds at windbreak half height where u is the wind speed, u_0 is the undisturbed wind speed, and H is the height of the windbreak (Lin et al., 2007a). The measured wind speed is taken from Eimern et al. (1964)

The model was also validated for odour concentration simulation (Fig. 9). The correlations between MAHT and SAHT for the 11 tests, as a function of distance from the source, were found to be statistically significant (P = 0.01), implying that the standard k-ε model can accurately predicts odour HT downwind from windbreaks. As illustrated in Figure 5 a, c, e, and g for tests 2, 5, 7, and 8, the simulated lines are found in the centre of the range of MAHT, which is a good indication that the model can reproduce the observations. Depending on the test, the R^2 value ranged between 0.48 and 0.90. If all values within 150 m

of the windbreak are excluded to remove the odour puff effect, then R^2 exceeds 0.75 for all simulations.
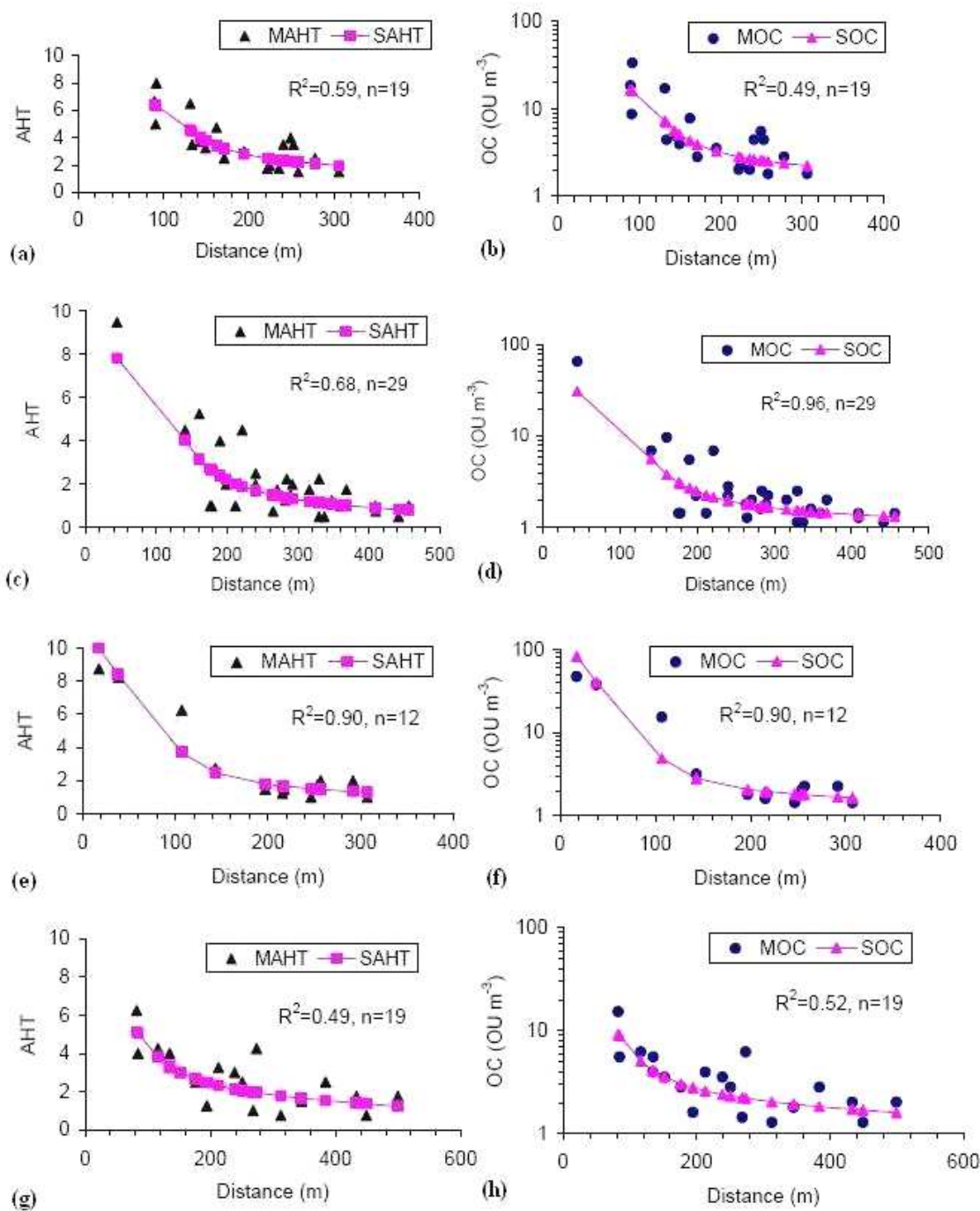

Fig. 9. For the field tests 2, 5 , 7 and 8, a, c, e, g give the measured and simulated absolute hedonic tone where *AHT* is the absolute hedonic ton, *MAHT* and *SAHT* are the measured and simulated hedonic tone, respectively, R^2 is the correlation coefficient between the *MAHT* and *SAHT* and n is odour points measured; b, d, f, h give the measured and simulated odour concentration where *OC* is odour concentration, *MOC* and *SOC* are respective measured and simulated *OC,* and R^2 is the correlation coefficient between *MOC* and *SOC*. The *x* axis indicates the distance from the odour source (Lin et al., 2009a)

4.4 Simulated effect of windbreak characteristics on odour dispersion

When establishing a natural windbreak to improve odour dispersion, the tree belt characteristics must be optimized in terms of porosity, height and distance from the source. The following sections will present results of simulations designed to identify the windbreak characteristics minimizing the size of the odour plume.

4.4.1 Windbreak porosity, tree type and height

The porosity is the main factor governing the amount of air flowing through the windbreak as determined by the inertial resistance coefficient C_{ir}, for given H, h_1, w_1, w_2, and w_3 values (Eqn 9, 10 and 11).

The following values were used to simulate conditions establishing optimal windbreak porosity: H and h_1 of 9.2 and 6.9 m; an aerodynamic porosity α of 0.2, 0.3 and 0.66 resulting in respective w_1, w_2, and w_3 values of 4.508, 3.864 and 0.644 for $a = 0.2$, values of 1.204, 1.032 and 0.172 for $a = 0.4$, and values of 0.38, 0.2598 and 0.16 for $a = 0.66$, and; an odour source 30 m upwind from the windbreak.

The simulation indicated that aerodynamic porosity is the main factor governing odour trapping behind the windbreak, and accordingly, odour dispersion and odour plume shortening (Fig. 10). As compare to α of 0.2 dropping the odour concentration to 2 OU m^{-3} at a distance of 217 m, a of 0.4 required a distance of 292 m to drop the odour concentration to the same level. For a of 0.66, a distance of over 452 m was required to reach the same OC of 1 OU m^{-3}. Furthermore and for aerodynamic porosities of 0.2, 0.4 and 0.6, the odour plume width measured 73, 37 and 30 m, respectively. Thus, lower aerodynamic porosities produced shorter but wider odour plumes, because of the trapping of more odours immediately downwind from the windbreak. Fig. 6 shows the effect of windbreak aerodynamic porosity on the profile of the odour dispersion plume. Again, the lower density windbreak produced a higher OC immediately downwind, confirming the enhanced trapping of odours before dispersion.

The tree type had a slight impact on odour plume length, for the same aerodynamic porosity. For example, a single row conifer produced an OC of 2 OU m^{-3} at 320 m, as compared to 310 m for the poplars. The velocity gradient created by the conifer windbreak gradually increased with height especially above 6.4 m as a result of the drop in horizontal tree section area, explaining its slightly poorer performance.

As for a tree height of 4.6 and 9.2 m, for a windbreak offering the same aerodynamic porosity of 0.4, an OC of 3 OU m^{-3} was reached at 225 and 407 m, respectively. The size of the low turbulence zone is thus directly related to the windbreak tree height.

4.4.2 Windbreak distance from the source

The simulations demonstrated that the shorter the distance between the source and the windbreak, the faster the odours are trapped to be concentrated and then dispersed. For the 15 m distance, the 2 OU m^{-3} contour occurred at a distance of 309 m from the source or 287 m from the windbreak, including its thickness. The 2 OU m^{-3} contour appeared for the 60 m distance, at a distance of 411 m from the source and 347 m from the windbreak. The 15 and 60 m distance between the source and windbreak resulted in simulated OC upwind from the windbreak of 228 and 73 OU m^{-3} respectively, at a height z = 1.5 m.

When the odour is released from a building ventilated naturally, the windbreak should be positioned at least 24 m away, a condition which does not necessarily optimise odour dispersion.
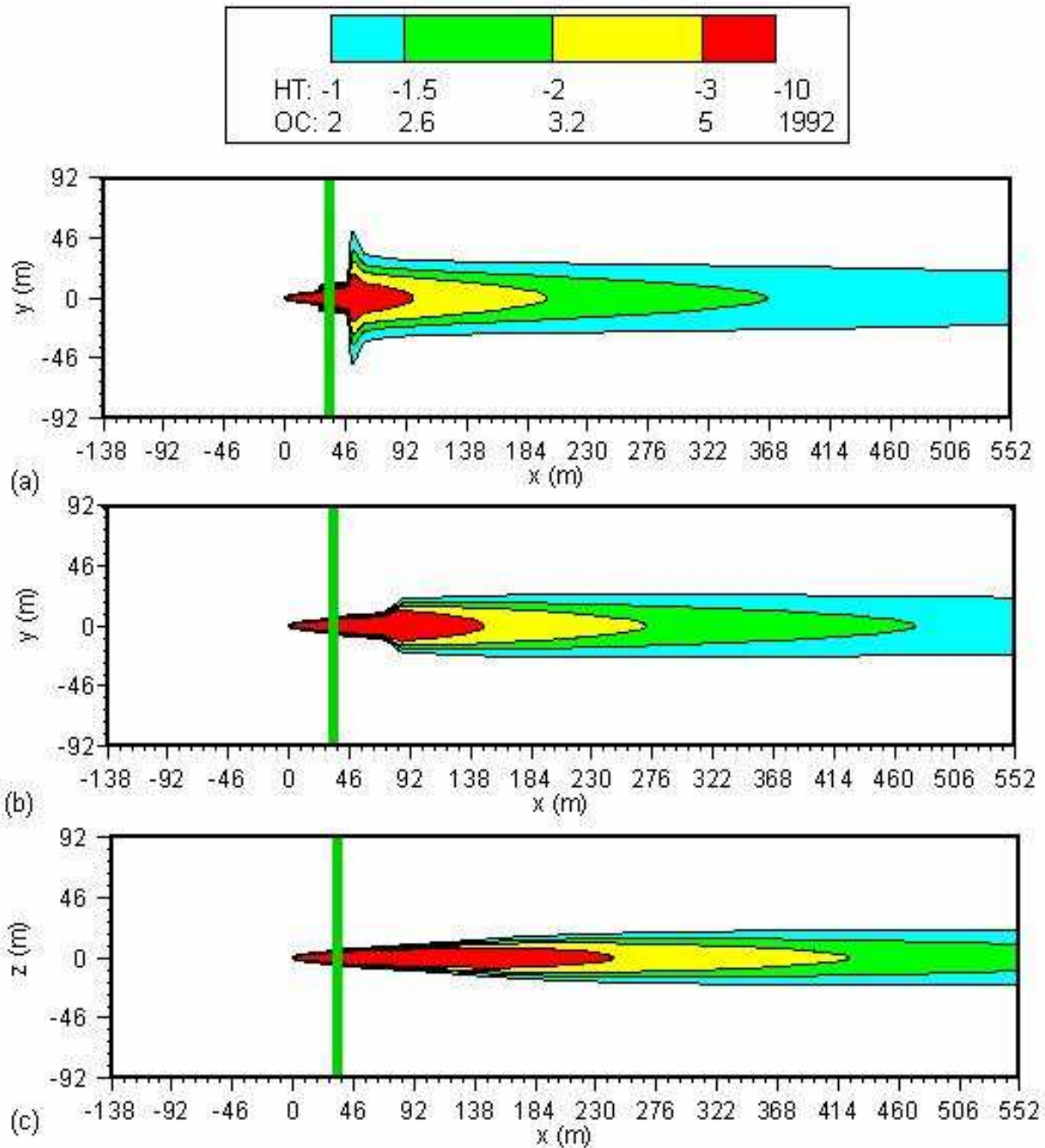

Fig. 10. Contours of the odour plume (z = 1.5 m) for an aerodynamic porosity of (a) 0.2, (b) 0.4 and (c) 0.66, respectively. The green bar is the windbreak and the unit of the odour concentration is OU m^{-3} (Lin et al., 2009a)

4.5 Simulated effect of climatic conditions on windbreak odour dispersion
Weather conditions certainly vary in time and affect the dispersion performance of a windbreak. Furthermore, atmospheric stability impacts the effect of climatic factors since it

represents the degree of air convection or air movement in the vertical direction. It can compete against wind and it defines air temperature gradient with height. Accordingly and when simulating the effect of the main climatic factors of wind velocity and air temperature, atmospheric stability must be examined in parallel.

4.5.1 Effect of wind velocity and direction

For unstable atmospheric stability conditions (Category B), wind velocities of 1.0, 1.8 and 3.0 m s^{-1} produced simulated odour plume length of 321 m, 406 m and 268 m for a 2 OU contour (Fig. 11). Accordingly, low wind velocity (1.0 m s^{-1}) could not counteract the air lifting effect of unstable conditions, as opposed to stronger winds carrying odours further. Similarly, the height of the odour plume decreased from 43 to 17 and 15 m with increasing wind velocities 1.0, 1.8 and 3.0 m s^{-1}, respectively.

For neutral atmospheric stability conditions (Category D) with wind velocities of 3.0, 5.4 and 6.4 m s^{-1}, the odour plume length decreased from 272 m to 121 and 102 m (Fig. 11) respectively, for a 2 OU m^{-3} contour .Wind velocities for neutral atmospheric conditions are normally higher than those associated with unstable conditions and produce a higher turbulence kinetic energy at the windbreak which enhances odour dispersion (Lin et al., 2007b). This is also reflected in terms of odour flux which is accelerated by the turbulence viscosity proportional to turbulent kinetic energy.

For stable atmospheric stability conditions (Category F) with typical wind velocities of 1.0, 1.9 to 3.0 m s^{-1}, the odour plume length dropped from 552 to 350 and 253 m, respectively. Under stable atmospheric conditions with limited upward convection, as compared to unstable conditions, vertical forces are not as strong and less air is projected upwards at the windbreak, resulting in lower wind velocities, weaker turbulent kinetic energy at the windbreak and therefore a longer odour plume.

Wind direction affects the orientation and shape of the odour plume. On the horizontal plane z = 1.5 m and for wind directions varying from 0 to -90°, the shape of the odour plume followed wind direction (Fig 12). The length of the odour plume decreased from 281 to 176 m for a wind direction changing from 0 to -45° and then increased from 176 to 321 m for a wind direction changing from -45 to -90°, for a 2 OU contour. The odour plume developed a fin immediately downwind from the windbreak when the wind direction ranged between -15 and -75°. This fin was generated when sufficient air flowed parallel to the windbreak and when the windbreak could sufficiently reduce the x-component of the air flow. At a distance of 28 m downwind from the windbreak, the wind streamlines were observed to sharply change direction and become parallel to the windbreak. As a result, the fin reached its maximum length when the wind direction was -45°.

4.5.2 Effect of atmospheric stability

Atmospheric stability condition had a major impact on odour plume length because it establishes wind velocity range and temperature gradient as well as the strength of the convective air forces. Assuming an average wind velocity, temperature and atmospheric boundary layer height, the odour plume length for an odour contour of 2 OU, measured 406, 170 and 350 m for unstable, neutral and stable atmospheric stability conditions (Categories B, D and F), respectively. Hence, OPL increased from Category D to B and

then F, because Categories B and F generally exhibit lower wind speeds compared to Category D.
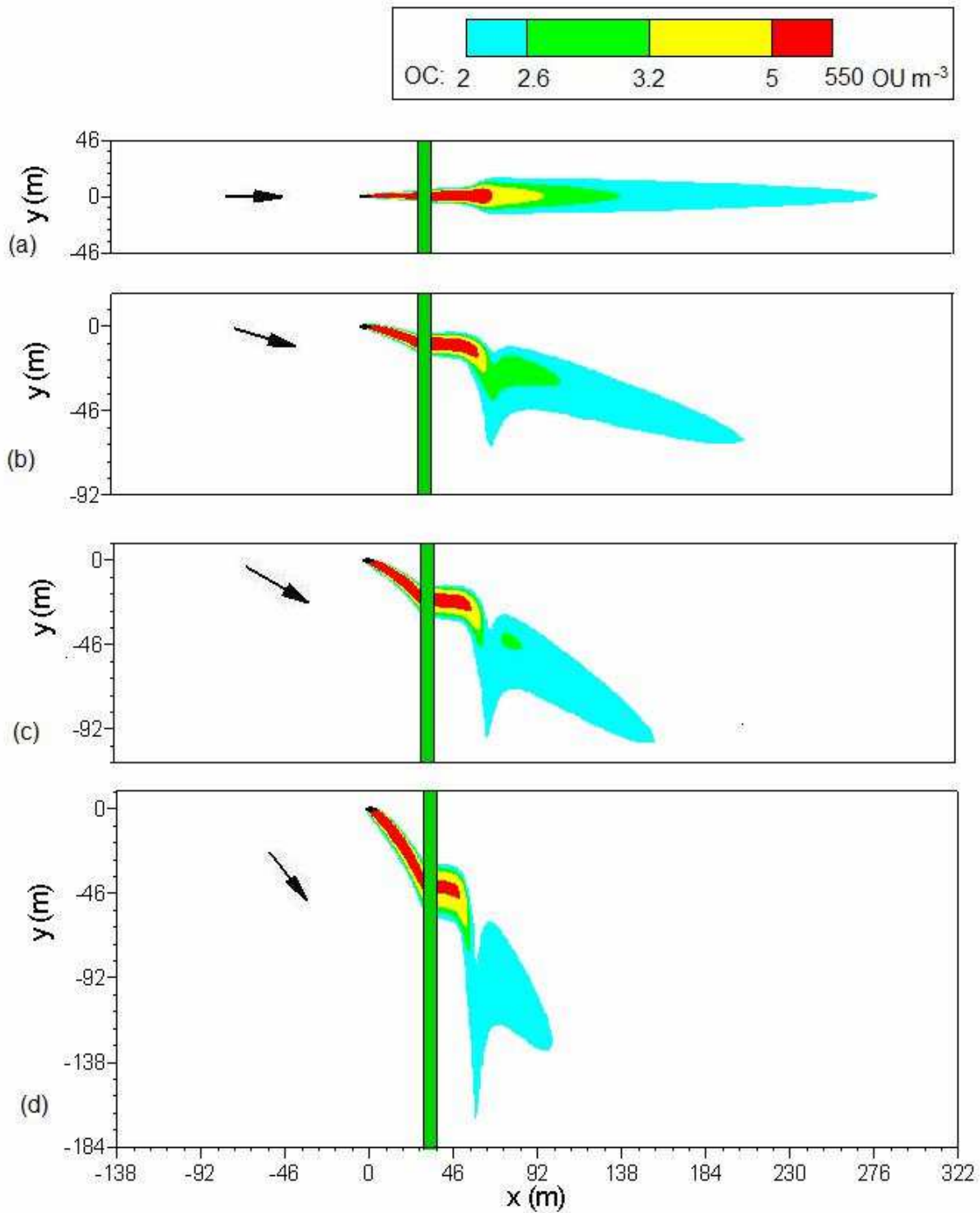
Fig. 11. Effect of wind velocity for: upper) unstable atmosphere for wind velocities of (a) 1.0 m s^{-1}; (b) 1.8 m s^{-1} , and; (c) 3 m s^{-1} ; lower) neutral atmosphere for wind velocities (a) 3 m s^{-1}; (b) 5.4 m s^{-1} , and; (c) 6.4 m s^{-1}. The green bar is the windbreak; the odour concentration is in OU m^{-3} (Lin et al., 2009b)
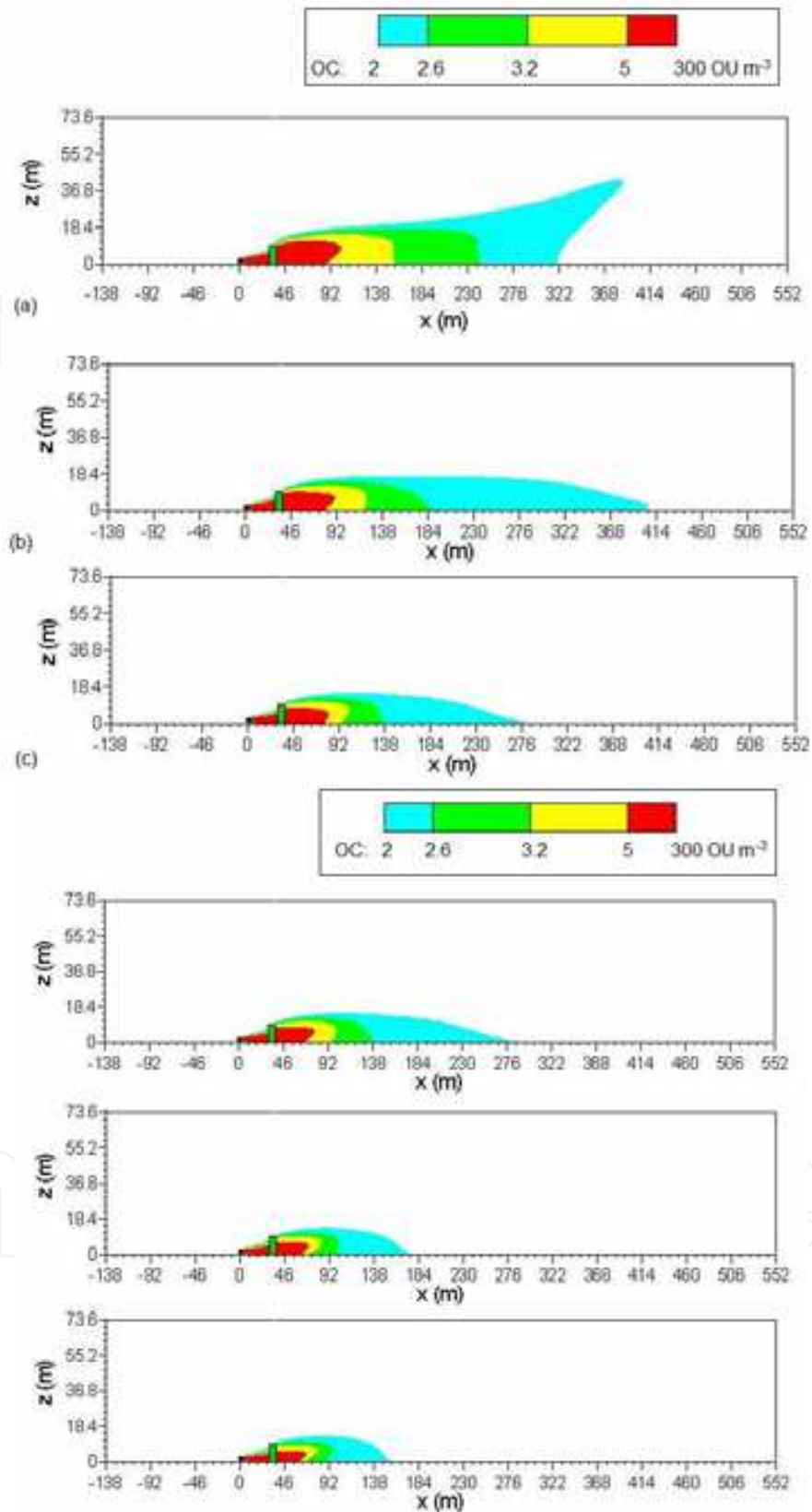
Fig. 12. Effect of wind direction on the odour plume for an horizontal plane at z = 1.5 m, when the wind direction from the positive x-axis is (a) 0˚; (b) 15˚; (c) 30˚, and; (d) 45˚. The green bar is the windbreak (Lin et al., 2009b)

For the same atmospheric boundary layer height, and wind velocity and air temperature at a height of 10 m, but for Stability Categories B, D and F, odour plumes measured in length 267, 272 and 253 m, respectively because of a different typical profile for wind velocity, temperature and turbulence. The turbulent kinetic energy on the upwind side of the windbreak decreases from Stability Category B, to that of D and then F but then increases in the opposite order on the downwind side of the windbreak, thus shortening the odour plume (Lin et al., 2007b).

For Stability Categories B, D and F, the vertical wind velocity profile was different for 3 m s^{-1} at a 10 m height. Stability Category B produced a profile slightly smaller than that obtained with Category D, but for Categories B and D, the profile was much smaller than that for Category F.

For a temperature of 291 K at a 10 m height, the vertical temperature profile was quite different for Stability Categories D, B and F. For Stability Category D (neutral conditions), this profile decreased with height at a rate 0.01 K m^{-1}, but for that of B (unstable conditions), it dropped much faster over a height of 0 to 10 m and then deceases at a slower rate but still faster than that obtained with Stability Category D. The temperature profile for Stability Category F (stable conditions) increased with height and produced the inverse of stable effects. Because Stability Category F produced larger profile differences for wind velocity and temperature, between heights of 0 and 73.6 m in the computational domain, compared to D and B, the resulting odour plume was shorter.

Generally, the odour plume length for neutral atmospheric conditions (Category D) was shorter than that for unstable (Category B) and stable conditions (Category F), because of the corresponding different wind velocity. However, when all the conditions were the same except for atmospheric stability conditions, Category F produced a slightly shorter odour plume compared to that under neutral and unstable conditions.

4.5.3 Effect of air temperature gradient

In general, the ground air temperature had limited effect on odour plume size, when associated with a specific atmospheric condition. On a horizontal plane with $z = 1.5$ m, same length odour plumes were obtained at temperatures of 293 and 269 K under unstable neutral and stable atmospheric conditions.

The phenomenon can be explained by the fact that the odour diffusion flux is proportional to ($\Delta T/T$) or the rate of change of temperature T. For neutral atmospheric conditions, T dropped with height at 0.01 K m^{-1}, but the rate of change of T over a 0 to 20 m height was similar in both cases at 0.069 % and 0.074 %, respectively. The differences for Simulations 2 and 10, and 8 and 12 of 0.006 % and 0.005 %, respectively, were too small to influence odour dispersion. Hence, the same odour plumes were observed for the different temperatures under the same atmospheric stability condition.

5. Conclusions

The objective of the project was to develop a model from the Computational Fluid Dynamics method based on SST k-ω computations (Fluent inc., 2005) to simulate odour dispersion around windbreaks and then to use this validated model to observe the effect on odour plume size of windbreak characteristics and climatic factors. The model was calibrated for odour dispersion using field data measured by panellists.

The simulations produced the following conclusions:

1. After calibration, the SST k-ω model simulated the velocity recovery rate observed downwind from a 2-dimensional windbreak with an R^2 factor of 0.95 for distances of 0 to 30 H, where H is the height of the windbreak;
2. The SST k-ω model predicted odour concentration with an R^2 value generally above 0.75 for values over 150 m away from the windbreak, which is considered quite acceptable for odour simulations.
3. A less porous or denser windbreak (aerodynamic porosity of 0.2 versus 0.4 and 0.66) produced a shorter, wider and more intense odour plume;
4. Assuming that the air flow resistance was proportional to the square of the tree diameter, the tree type had almost no effect on the size of the odour plume. As opposed to the conifer, the poplar windbreak created a slightly shorter odour plume for the same aerodynamic porosity;
5. A taller windbreak resulted in a shorter odour plume, by creating a taller low turbulence zone downwind from the windbreak, where more odours were trapped and retained for dispersion;
6. When close to odour source, the windbreak produces a shorter odour plume.
7. In terms of climatic factors, atmospheric stability was the governing element since it generally establishes wind speed and air temperature gradient; under low wind speeds weaker than convective forces, the odour plume was shorter but under low convective forces, higher wind speeds created more turbulences and shorter odour plumes.

6. Nomenclature

AHT is absolute hedonic tone

AS is atmospheric stability

a_s is a factor involved in determining TKE

C_{ir} is the inertial resistance coefficient

C_{ir0} is the constant

C_p is specific heat of air

D_1 and D_2 are the tree diameters

$D_{i,m}$ is the diffusion coefficient for species i in the gaseous mixture

$D_{T,i}$ is the thermal diffusion coefficient for species i in the gaseous mixture

DWO is the distance between the windbreak and the odour source

E is the total energy

F_i is the resistance to wind flow

g is acceleration of gravity

g_i is the component of the gravitational vector in the ith direction

H is the total height of the windbreak

H_F is the vertical heat flux

h_i is the height at which the rate of the gradient of the tree diameter changed at the ith height

h_{ABL} is the height of the atmospheric boundary layer

H_i is the sensible enthalpy of ith species

HT is the odour hedonic tone

J_i is the diffusion flux of species i

k_a is the van Karman constant ranging from 0.35 to 0.43, and n9ormally equal to 0.4

k is the turbulence kinetic energy

k_{eff} is the effective thermal conductivity

$k(z)$ is the turbulence kinetic energy (TKE)

l is the turbulence length scale

L_{MO} is the Monin Obukhov length

M is the molecular weight of dry air (0.028966kg mol^{-1})

m_{H2S} is the mass of hydrogen sulphide in one odour unit

OC is the odour concentration in OU m^{-3}

OC_g is the odour concentration at odour generator in OU m^{-3}

ODS is the odour dispersion system used for simulations

OER is the odour emission rate

OMF is odour mass fraction, dimensionless

p is the static pressure

P_a is the atmospheric pressure at sea level

R is the universal gas constant (8.31432J mol^{-1} K^{-1})

$SAHT$ is simulated absolute hedonic tone

Sc_t is the turbulent Schmidt number generally equal to 0.7

S_h is the heat of chemical reaction and other volumetric heat sources

SOC is simulated odour concentration in OU m^{-3}

$SOMC$ is odour mass concentration in µg m^{-3}

T is temperature

TKE is turbulence kinetic energy

T_s is the temperature at the z_s

$T_{(z)}$ is the vertical temperature profile

T_{WC} is a factor to control the convective energy varied with height

T_{WN} is a factor controlling the drop in TKE with height within the atmospheric boundary layer

t is time

$\mathbf{u}$ is instantaneous wind velocity

u and u' are mean and fluctuating component of instantaneous velocity

u_* is the friction velocity

u_i (i=1, 2, 3) is scalar component of the mean velocity in ith direction, indicating in x, y, z direction in Cartesian coordinate system, respectively

u_i' (i=1, 2, 3) is the fluctuating component of the instantaneous velocity ith direction, indicating in x, y, z direction in Cartesian coordinate system, respectively

u_{mag} is magnitude of the mean velocity

u_0 is the undisturbed wind velocity

w_* is the mixing layer velocity scale

$w_{(z)}$ is the vertical turbulence specific dissipation rate

w_1, w_2, w_3 are constant describing the tree shape and resistance to wind flow at a height h_1, h_2, h_3 respectively

x is the coordinate for the axis perpendicular to the windbreak

y is the coordinate for the axis parallel to the windbreak

z is the coordinate for the vertical axis

z_0 is roughness length

z_s is a height of 1.35 m above surface

Y_i is the mass fraction of the species i in a mixture of gases

Y_2 is the odour mass fraction

z is a coordinate in the vertical direction

a is the aerodynamic porosity, or permeability

a^{-1} is the viscous resistance coefficient

β is the optical porosity

μ is viscosity of mixture of the air and odorous gases

μ_t is the turbulence kinetic viscosity

ρ is fluid density

ω is the specific dissipation rate

δ_{ij} is the unit tensor

$(\tau_{ij})_{eff}$ is the effective deviatoric stress tensor

σ_u, σ_v and σ_w are the turbulence components in x, y, z coordinates

Y_d is dry adiabatic lapse rate of 0.01 K m^{-1}

7. Acknowledgment

8. References

ASHRAE. (2009). *Handbook of Fundamentals*. American Society of Heating, Refrigeration and Air Conditioning, Atlanta, Georgia, U.S.A, pp.13.1-13.6.

ASTM (1997a). *Standard Practice for Defining and Calculating Individual and Group Sensory Thresholds from Forced-Choice Data Sets of Intermediate Size*. E1432-91. West Conshohocken, PA, American Standards of Testing and Measurement International.

ASTM (1997b). *Standard Practice for Determination of Odour and Taste Thresholds by a Forced-Choice Ascending Concentration Series Method of Limits*. E679-91. West Conshohocken, PA, American Standards of Testing and Measurement International.

ASTM (1999). *Standard practice for referencing supra-threshold odour intensity*. E544-75. Philadelphia, Pa, USA, American Standards of Testing and Measurement International.

Bird, R.B.; Stewart, W.E & Lightfoot, E.N. (2002). *Transport phenomena*. John Wiley, New York, USA.

Blackadar, A.C. (1997). *Turbulence and diffusion in the atmosphere: lectures in environmental sciences*. Springer Berlin Publishers, New York, USA.

Bottcher, R.W.; Munilla, R.D.; Baughman, G.R. & Keener, K. M. (2000). Designs for windbreak walls for mitigating dust and odour emissions from tunnel ventilated swine buildings. In: *Swine Housing, Proc. of the 1st International Conference*, Oct. 9-11, 2000, Des Moines, Iowa. American Society of Agricultural Engineers, 2950 Niles road, St. Joseph, Mi. USA. pp. 174-181.

Bottcher, R.W.; Munilla, R.D.; Keener, K.M. & Gates, R.S. (2001). Dispersion of livestock building ventilation using windbreaks and ducts. *2001 ASAE Annual International Meeting,*paper 01-4071. 2950 Niles Road, St. Joseph, Mi. USA.

Carruthers, D.J. & Dyster, S.G. (2006). *Boundary layer structure specification*. ADMS 3 P09/01T/03 http://www.cerc.co.uk/software/pubs/3-1techspec.htm visited in April 2006.

Cavalini, P. M.; Koeter-Kemmerling, L. G. & Pulles, M. P. J. (1991). Coping with odour annoyance and odour concentratioons: three field studies. *Journal of Environmental Psychology*, Vol. 11, pp.123-142.

CEN (2001). *Air quality - determination of odour concentration by dynamic olfactometry*. prEN13725. 36 rue de Stassart, B-1050 Brussels, European Committee for Standardization.

Chen, Y. C.; Bundy, D. S.; Hoff, S. (1998). Development of a model of dispersion parameters for odour transmission from agricultural sources. *Journal of Agricultural Engineering Research*, Vol. 69,pp. 229-238.

Choinière, D. & Barrington, S. (1998). The conception of an automated dynamic olfactometer. *CSAE/SCGR* paper 98-208. Winnipeg, Manitoba, Canada.

Das, K.C.; Kastner, J.R.& Hassan, S.M. (2004). Potential of particulate matter as a pathway for odour dispersion. *ASAE paper 04-4125*. American Society of Agricultural Engineering, St Joseph, Michigan, USA.

Edeogn, I.; Feddes, J.J.R.; Qu, G.; Coleman, R. & Leonard, J. (2001). *Odour measurement and emissions from pig manure treatment/storage systems*. Final report, University of Alberta, Edmonton, Canada.

Eimern, J.V.; Karschon, R.; Razumova, L.A. & Robertson, G.W. (1964).*Windbreak and shelter belts*. Report of a working group of the Commission for Agricultural Meteorology, World Meteorological Organization, Technical note 59, Secretariat of the World Meteorological Organization, Geneva, Switzerland.

Evans, G. W. & Cohen, S. (1987). *Environmental stress*. In D. Stokols & I. Altman Eds., Handbook of Environmental Psychology, New York: Wiley, pp. 571-610.

Fluent inc. (2005). Fluent 6.2 user's guide. Fluent Inc., Centerra Resource Park, Lebanon, NH, USA.

Fox, R.W. & McDonald, A.T. (1992). *Introduction to fluid mechanics*. John Wiley, New York, USA.

Gassman, P. W. (1993). Simulation of odour transport: A review. *ASAE Paper 92-4517*. St Joseph, Michigan, USA, American Society of Agricultural Engineering.

Golder, D. (1972). Relations among stability parameters in the surface layer. *Boundary-Layer Meteorology*, Vol. 3, pp.47.

Guan, D.; Zhang, Y. & Zhu, T. (2003). A wind-tunnel study of windbreak drag. *Agriculture, Ecosystem & Environment*, Vol. 118, pp.75-84.

Guo, Y.; Jacobson, L. D.; Schmidt, D. R. & Nicolai, R. E. (2001). Calibrating INPUFF-2 model by resident-panellists for long-distance odour dispersion from animal production sites. *Transactions of the ASAE*, Vol. 17, pp.859-868.

Heisler, G.M. & Dewalle, D.R. (1988). Effects of windbreak structure on wind flow. *Agriculture, Ecosystems and Environment*. Vol. 22-23, pp.41-69.

Hinze, J.O., 1975. Turbulence, McGraw-Hill, New York, USA.

Jacob, T. J. C.; Fraser, C.; Wang, L.; Walker, V. & O'Connor, S. O. (2003) Psychophysical evaluation of responses to pleasant and mal-odour stimulation in human subjects; adaptation, dose response and gender differences. *International Journal of Psychophysiology*, Vol. 48, pp.67-80.

Jacobson, L. D.; Guo, H.; Schmidt, D. R.; Nicolai, R .E.; Zhu, J. & Janni, K. A. (2005). Development of the OFFSET model for determination of odour annoyance free setback distances from animal production sites: Part I. Review and experiment. *Transactions of the ASAE*, Vol. 48, pp.2259-2268.

Jacobson, M.Z. (1999). *Fundamentals of atmospheric modeling*. Cambridge University Press, Cambridge, UK.

Le, P. D.; Aarmink, A. J. A.; Ogink, N. W. M. & Verstegen, M.W. A. (2005). Effect of environmental factors on odour emission from pig manure. *Transactions of the ASAE*, Vol. 48, pp.757-765.

Li ,Y. & Guo, H. (2008). Evaluating the effect of computational time steps on livestock odour dispersion using a CDF model. *Transcations of the ASABE*, Vol. 50, pp.2199-2204.

Lim, T.T.; Heber, A.J.;Ni, J.Q.; Sutton, A.L. Sutton & Kelly, D.T.(2001). Characteristics and emission rates of odour from swine nursery buildings. *ASBE Transactions*, Vol. 44, pp. 1275-1282.

Lin, X.-J.; Barrington, S.; Nicell, J. & Choinière, D. (2009). Evaluation of standard k-ε model for the simulation of odour dispersion downwind from windbreaks. *Canadian Journal of Civil Engineering*. Vol. 36, pp. 895-910.

Lin, X.J.; Choinière, D. & Prasher, S. & Barrington, S. (2009b). Effect of weather on windbreak odour dispersion. *Journal of Wind Engineering and Industrial Aerodynamics*, Vol 97, pp.487-496. ISSN: 0167-6105.

Lin, X.-J.; Nicell ,J.; Choinière, D.; Vézina, A. & Barrington, S. (2006). Field odour dispersion plume produced by different natural windbreaks. *Journal of Agriculture, Ecosystems & Environment*, Vol. 116, pp. 263-272. ISSN: 0167-8809.

Lin, X.-J.; Nicell, J.; Choinière, D. & Barrington, S. (2007b). Simulation of the effect of windbreak characteristics on odour dispersion. *Biosystems Engineering*, Vol. 98, pp. 347-363. ISSN: 1537-5110.

Lin, X.-J.; Nicell, J.; Choinière, D. & Barrington, S. (2007c). Effect of natural windbreaks on maximum odour dispersion distance. *Journal of Canadian Biosystems Engineering*, Vol. 49, pp.6.21-6.32.

Lin, X.-J.; Nicelle, J.; Choinière, D. & Barrington, S. (2007a). Livestock odour dispersion as affected by natural windbreaks. *Journal of Soil, Water and Air Pollution*, Vol 182, pp.263-273.

McPhail, S. (1991). Modeling the dispersion of agricultural odours . *Proceedings of a workshop on agricultural odours*. Toowoomba, Queensland, Australia. AMLRDC Report No. DAQ 64/7. Feedlot Services Group, Queensland Department of Primary Industries. Toowoomba, Queensland, Australia.

Menter, R.R.; Kuntz, M. & Langtry, R. (2003). Ten years of industrial experience with the SST turbulence model. In: K. Hanjalic, Y. Nagano and M. Tummers (Editors), Turbulence, Heat and Mass Transfer 4. Begell House Inc, Redding, CT, pp.625-632.

Nimmermark, S. (2006). *Characterization of odour from livestock and poultry operation by the hedonic tone*. Paper number 064157. In: ASABE Annual International Meeting,

American Society of Agricultural and Biological Engineering, St Joseph, Michigan, USA.

O'Neill, D.H. & Phillips, V.R. (1992). A review of the control of odour nuisance from livestock buildings: Part 3, properties of the odorous substances which have been identified in livestock wastes or in the air around them. *Journal of Agricultural Engineering Research*, Vol. 53, pp.23-50.

Panofsky, H.A. & Dutton, J.A. (1984). *Atmospheric turbulence: models and methods for engineering applications*. Wiley, New York, USA.

Plate, E.J., 1971. The aerodynamics of shelter belts. *Agricultural Meteorology*, Vol. 8, pp203.

Redwine, J. S. & Lacey, R. E. (2000). A summary of state-by-state regulation of livestock odour. In: *Proceedings of the Second International Conference on Air Pollution from Agricultural Operations*, St. Joseph, Michigan, ASBE.

Riddle, A.; Carruthers, D.; Sharpe, A.; McHugh, C. & Stocker, J. (2004).Comparisons between FLUENT and ADMS for atmospheric dispersion modelling. *Atmospheric Environment* ,Vol. 38, pp.1029-1038.

Saatdjian, E.B. (2000). *Transport phenomena: equations and numerical solutions*. John Wiley, New York, USA.

Sarkar, U.; Longhurst, P. J. & Hobbs, S. E. (2002). Community modeling: a tool for correlating estimates of exposure with perception of odour from municipal solid waste landfills. *Journal of Environmental Management*,Vol. 68, pp.153-160.

SAS Institute Inc. (2001). *SAS (r) Proprietary Software Release 8.2*. SAS, Cary, NC, USA.

Schauberger, G.; Piringer, M. & Petz, E. (1999). Diurnal and annual variation of odour emission from animal houses: a model calculation for fattening pigs. *Journal of Agricultural Engineering Research*, Vol. 74, pp.251-259.

Schnelle, K.B. & Dey, P.R. (2000). *Atmospheric dispersion modeling compliance guidelines*. McGraw-Hill, New York, USA.

Smith, R. J. & Watts, P. J. (1994). Determination of odour emission rates from cattle feedlots: Part 1, A review. *Journal of Agricultural Engineering Research*, Vol. 57, pp.145-155.

Sun, H.; Stowell, R.R.; Keener, H. M. & Michel, F.C. (2002). Comparison of predicted and measured ammonia distribution in a high-rise™ hog building (HRHB) for summer conditions. *Transactions of the ASAE*, Vol. 45, pp.1559-1568.

Ucar, T. & Hall, F.R. (2001). Review windbreaks as a pesticide drift mitigation strategy: a review. *Pest Management Science*, Vol. 57, pp.663-675.

Vigiak, O.; Sterk, G.; Warren, A. & Hagen, L.J. (2003). Spatial modeling of wind speed around windbreaks. *Catena*, Vol. 52, pp.273-288.

Wang, H. & Takle, E.S. (1997). Momentum budget and shelter mechanism of boundary-layer flow near a shelterbelt. *Boundary-Layer Meteorology*, Vol. 82, pp.417-435.

Wang, H.; Takle, E. S. & Takle, A. (1995). Numerical simulation of boundary-layer flows near shelterbelt. *Boundary-Layer Meteorology*, Vol. 75, pp.141-173.

Wilson, J.D. & Yee, E. (2003). Calculation of winds distribution by an array of fences. *Agricultural and Forest Meteorology*. Vol. 115,pp. 31-50.

Wilson, J.D. (1985). Numerical study of flow through a windbreak. *Journal of Wind Engineering and Industrial Aerodynamics*, Vol. 21, pp.119-154. ISSN: 0167-6105.

Wilson, J.D. (2004). Oblique, stratified winds about a shelter fence. Part II: Comparison of measurements with numerical models. *Journal of Applied Meteorology*, Vol. 43, pp.1392-1409.

Xing, Y.; Guo, Y.; Feddes, J. & Shewchuck, S. (2006). Evaluation of air dispersion models using swine odour plume measurement data. *CSAE Paper 06-172*. Canadian Society of Agricultural Engineering, Winnipeg, Manitoba, Canada.

Zald, D. H. & Pardo, J. V. (2000). Functional neuroimaging of the olfactory system in humans. *International Journal of Psychophysiology*, Vol. 36, pp.1165-1181.

Zhang, Q.; Feddes, J.; Edeogu, I.; Nyachoti, M.; House, J.; Small, D.; Liu, C.; Mann, D. & Clark, G. (2002). *Odour production, evaluation and control*. Manitoba Livestock manure Management Initiative Inc., Winnipeg, Manitoba, Canada.

Zhang, Q.; Zhou, X. J.; Cicek, N. & Tenuta, M. (2007). Measurement of odour and greenhouse gas emissions in two swine farrowing operations. *Canadian Biosystems Engineering*, Vol. 49, pp.6.13-6.20.

Zhu, J.; Jacobson, L. D.; Schmidt, D. R. & Nicolai, R. (2000). Evaluation of INPUFF-2 model for predicting downwind odours from animal production facilities. *Applied Engineering in Agriculture*, Vol. 16, pp.159-164.
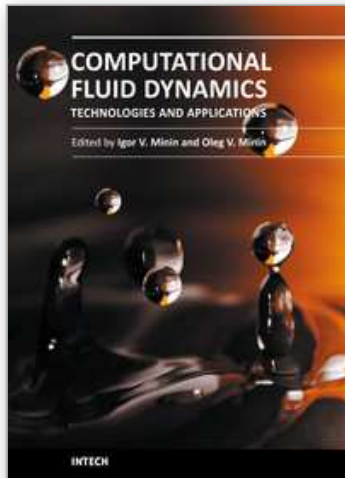
Computational Fluid Dynamics Technologies and Applications

Edited by Prof. Igor Minin

ISBN 978-953-307-169-5

Hard cover, 396 pages

Publisher InTech

Published online 05, July, 2011

Published in print edition July, 2011

This book is planned to publish with an objective to provide a state-of-art reference book in the area of computational fluid dynamics for CFD engineers, scientists, applied physicists and post-graduate students. Also the aim of the book is the continuous and timely dissemination of new and innovative CFD research and developments. This reference book is a collection of 14 chapters characterized in 4 parts: modern principles of CFD, CFD in physics, industrial and in castle. This book provides a comprehensive overview of the computational experiment technology, numerical simulation of the hydrodynamics and heat transfer processes in a two dimensional gas, application of lattice Boltzmann method in heat transfer and fluid flow, etc. Several interesting applications area are also discusses in the book like underwater vehicle propeller, the flow behavior in gas-cooled nuclear reactors, simulation odour dispersion around windbreaks and so on.

How to reference

In order to correctly reference this scholarly work, feel free to copy and paste the following:

Barrington Suzelle, Lin Xing Jun and Choiniere Denis (2011). Simulating Odour Dispersion about Natural Windbreaks, Computational Fluid Dynamics Technologies and Applications, Prof. Igor Minin (Ed.), ISBN: 978-953-307-169-5, InTech, Available from: http://www.intechopen.com/books/computational-fluid-dynamics-technologies-and-applications/simulating-odour-dispersion-about-natural-windbreaks

INTECH

open science | open minds